TÜRKİYE CUMHURİYETİ
ADANA ALPARSLAN TÜRKEŞ SCIENCE AND TECHNOLOGY UNIVERSITY

GRADUATE SCHOOL
BIOENGINEERING DEPARTMENT

THE COMPARISON OF T98G CELL RESPONSE TO TRIFLUOPERAZINE in 2D & 2.5D MICROENVIRONMENT

GÖZDE GÜLDAĞ

M.Sc.

ADANA 2023

TÜRKİYE CUMHURİYETİ
ADANA ALPARSLAN TÜRKEŞ SCIENCE AND TECHNOLOGY UNIVERSITY

GRADUATE SCHOOL
BIOENGINEERING DEPARTMENT

THE COMPARISON OF T98G CELL RESPONSE TO TRIFLUOPERAZINE in 2D & 2.5D MICROENVIRONMENT

GÖZDE GÜLDAĞ

M.Sc.

THESIS ADVISOR
ASST. PROF. DR. MERVE ÇAPKIN YURTSEVER

ADANA, 2023

DECLARATION OF CONFORMITY

In this thesis study, which was prepared following the thesis writing rules of Adana Alparslan Türkeş Science and Technology University Institute of Graduate School, I declare that I provide all the information, documents, evaluations and results in accordance with scientific ethics and moral codes without resorting to any means or assistance that would be contrary to scientific ethics and traditions. I also declare that I refer to all of the articles I used in this study with appropriate references and accept all moral and legal consequences if a situation is found contrary to my statement regarding my work.

21/06/2023

Gözde GÜLDAĞ

ÖZET

TRİFLUOPERAZİN İLACININ T98G GLİOBLASTOMA HÜCRE HATTI ÜZERİNDEKİ ETKİSİNİN 2 BOYUTLU & 2.5 BOYUTLU ORTAMLARDA İNCELENMESİ

Gözde GÜLDAĞ

Yüksek Lisans, Biyomühendislik Anabilim Dalı

Danışman: Dr. Öğr. Üyesi Merve ÇAPKIN YURTSEVER

Haziran 2023, 48 sayfa

Kanser-ilaç etkileşimlerini inceleyen çalışmalarda, 3D kültür sistemlerinin canlı organizmalardaki koşulları 2D kültür ortamından daha iyi taklit ettiği gösterilmiştir. 2.5D hücre kültürü ortamları, 3D hücre kültürlerinden yararlanmak ve dezavantajlarını azaltmak için geliştirilmiş kültürlerdir. Trifluoperazin (TFP), şizofreniyi tedavi etmek için kullanılan FDA onaylı bir antipsikotik ve antiemetik ilaçtır. Farklı kanser hücrelerinin çoğalmasını ve istilasını engellediği ve çeşitli kanser hücre hatlarında ve hayvan modellerinde hücre ölümüne neden olduğu gösterilmiştir. T98G hücreleri, bir insan glioblastoma hücre hattıdır ve rutin olarak kanser tedavi yöntemlerini geliştirmek için deneysel modeller olarak kullanılır. TFP ilacının T98G hücre hattı üzerindeki etkisini 2D ortamda inceleyen sınırlı sayıda çalışma mevcuttur.

Bu tez çalışmasında, ilaç moleküllerinin *in vitro* olarak ucuz, hızlı ve *in vivo* hücre yanıtlarına daha benzer olmasını sağlayan bir kültür ortamı üretmesi amaçlanmıştır. T98G glioblastoma hücre dizisi, 2.5D ve 2D hücre kültürü sistemlerinde Trifluoperazin (TFP) varlığında ve yokluğunda hücre canlılığı ve morfolojisi açısından incelenmiştir. 2.5D hücre kültür sistemi için, genipin ve gliserolfosfat ile çapraz bağlı kitosan jeller üretilmiş ve T98G hücreleri doğrudan bu ıslak jeller üzerinde kültüre edilmiştir. Jellerin yüzey gözenek yapısı taramalı elektron mikroskobu ile incelenmiştir. Hücrelerin 2D ve 2.5D kültür sistemlerinde Trifluoperazin (1 µM, 2 µM, 4 µM, 6 µM ve 8 µM) ilaç molekülüne tepkisi, hücre canlılığının MTT analizi ve resazurin yöntemleri ile araştırılmıştır. Hücre çekirdeğinde meydana gelen değişimler DAPI boyama ile gösterilmiştir.

TFP'nin T98G hücre hattı üzerindeki IC50 konsantrasyonları, TCPS üzerinde 2D kültür için MTT analizi ile 24 saat için 3,75 μM ve 48 saat için 2,57 μM olarak hesaplanmıştır. TFP'nin T98G hücre hattı üzerindeki IC50 konsantrasyonları, TCPS üzerindeki 2D kültür için resazurin analizi ile 24 saat için 2.86 μM ve 48 saat için 2.64 μM olarak hesaplanmıştır. MTT ve resazurin analiz sonuçlarından hesaplanan IC50 konsantrasyonlarının çok yakın olduğu sonucuna varılmıştır. DAPI boyaması da TFP'nin 24 saatlik uygulamasından sonra T98G hücrelerinde kontrol grubuna kıyasla yoğunlaşmış ve küçük çekirdek şeklini göstermiştir. 2.5D kitosan hidrojel üretimi için çözücü olarak %0,5 asidik asit, fiziksel ve kimyasal çapraz bağlayıcı olarak 100 μL gliserol fosfat (1 g/mL) ve 1 mM genipin seçilmiştir. T98G hücreleri 24 ve 48 saat boyunca bu hidrojeller üzerinde kültüre edilmiştir. Hücrelerin canlılığı resazurin analizi ile belirlenmiştir. 2.5D kitosan hidrojeller üzerinde kültüre edilen T98G hücreleri için TFP'nin IC50 konsantrasyonu 24 saatlik kültür için 2.37 μM ve 48 saatlik kültür için 1.94 μM olarak belirlenmiştir.

Yapılan çalışmalar sonunda, 2.5D'de üretilen hidrojellerin, 3D hücre kültürü ortamını taklit ettiği görülmüştür. 2.5D boyutlu hidrojeller üzerinde kültüre edilen hücrelerin IC50 dozunun 2D TCPS üzerinde kültüre edilen hücrelerin IC50 değerine göre daha düşük ve yakın çıkması T98G hücrelerinin 2.5D hidrojeller üzerinde TFP ilacına daha duyarlı olabilceğini göstermiştir. Sonuçlar üretilen hidrojellerin hücreler için *in vitro* ve *in vivo* benzeri kültür koşullarının oluşturulduğunu ve hücre-ilaç yanıtının *in vivo*'ya göre daha yakından incelenebileceğini göstermiştir.

Anahtar Kelimeler: Glioblastoma, T98G, Trifluoperazin, 2.5D kitosan hidrojel

ABSTRACT

THE COMPARISION OF T98G CELL RESPONSE TO TRIFLUOPERAZINE in 2D & 2.5D MICROENVIRONMENT

Gözde GÜLDAĞ
M.Sc., Department of Bioengineering

Supervisor: Asst. Prof. Dr. Merve ÇAPKIN YURTSEVER
June 2023, 48 pages

In cancer-drug interaction studies, 3D culture systems have been shown to mimic living organism conditions better than 2D culture environments. 2.5D cell culture environments have been developed to take advantage of 3D cell culture and mitigate its disadvantages. Trifluoperazine (TFP) is an FDA-approved antipsychotic and antiemetic drug used to treat schizophrenia. It has been shown to inhibit the proliferation and invasion of various cancer cells and to induce cell death in several cancer cell lines and animal models. T98G cells are a human glioblastoma cell line and are routinely used as an experimental model for the development of cancer therapies.

There is a limited number of studies investigating the effect of TFP drug on T98G cell line in 2D culture. The aim of this thesis was to create an in vitro culture system for drug molecules that is cost-effective, efficient, and more similar to *in vivo* cell responses. The T98G glioblastoma cell line was evaluated for cell viability and morphology in the presence and absence of trifluoperazine (TFP) in 2.5D and 2D cell culture systems. For the 2.5D cell culture system, chitosan hydrogels cross-linked with genipin and glycerol phosphate were prepared and T98G cells were cultured directly on these wet hydrogels. The surface pore structure of the gels was examined by scanning electron microscopy. The response of the cells to Trifluoperazine (1 µM, 2 µM, 4 µM, 6 µM and 8 µM) drug molecule in 2D and 2.5D culture systems, cell viability was investigated by MTT assay and rezazurin methods. Changes in the cell nucleus were detected by DAPI staining.

The IC50 concentrations of TFP on T98G cell line was calculated as 3.75 μM for 24 h and 2.57 μM for 48 h by MTT analysis for 2D culture on TCPS. IC50 concentrations of TFP on T98G cell line was calculated as 2.86 μM for 24 h and 2.64 μM for 48 h by resazurin analysis for 2D culture on TCPS. It was concluded that, IC50 concentrations calculated from MTT and resazurin analysis results were very close. DAPI staining also showed the condensed and small nuclei shape in T98G cells after 24 h application of TFP when compared to the control group. According to these results TFP doses were selected as 1-8 μM for 2.5D cell culture studies. 2.5D chitosan hydrogels were prepared using 0.5% acidic acid as a solvent, 100 μL glycerol phosphate (1 g/mL) and 1 mM genipin as physical and chemical crosslinkers. T98G cells were cultured on these hydrogels for 24 and 48 h. Viability of the cells were both determined by resazurin analysis. IC50 concentration of TFP for T98G cells cultured on 2.5D chitosan hydrogels were determined as 2.37 μM for 24 h culture and 1.94 μM for 48 h culture.

In conclusion, it was observed that 2.5D chitosan hydrogels mimicked the 3D cell culture environment. The IC50 dose of cells cultured on 2.5D chitosan hydrogels was lower and closer to the IC50 value of cells cultured on 2D TCPS, indicating that T98G cells may be more sensitive to TFP drug on 2.5D hydrogels. The results showed that the hydrogels produced created *in vitro* and *in vivo*-like culture conditions for the cells and that the cell-drug response can be examined more closely than *in vivo*.

Keywords: Glioblastoma, T98G, Trifluoperazine, 2.5D chitosan hydrogel

Dedication

Dedication to my mother and father, whom I love dearly

To my family who have supported me so far.

ACKNOWLEDGEMENTS

I would like to thank everyone who helped me in my thesis with the pride of completing this thesis with difficulties.

First of all, I would like to thank my esteemed advisor, Asst.Prof.Merve Çapkın Yurtsever, who supported and guided me in all stages of my thesis and always supported me in my difficult times. I would like to thank my thesis committee members, Prof Dr. Mehmet Bertan Yılmaz and Asst. Prof. Özgür Cem ERKİN, your ideas and feedback will intellectually contribute to my development.

I would like to thank research assistant Selin Tünk and research assistant Meryem Damla Özdemir, who are both my teachers and spiritual sisters, who I could call no matter what time of day during this difficult process and never spared their help.

I thank all my lab mates; Dila Kurtul, Alican Cömertpay who were always helping me.

I would like to thank my mother and father who supported me throughout my life, and my uncles Hasan BAYDAR and Hüseyin BAYDAR, who became fathers when appropriate.

Thanks to TÜBİTAK for awarding me a National Scholarship in Priority Fields in Science 2210/C Fellowship, providing me with the financial means to complete this thesis.

This thesis was financially supported by ATU BAP Coordination Unit with project number of 21303016.

TABLE OF CONTENTS

LIST OF FIGURES

LIST OF TABLES

LIST OF ABBREVIATIONS

2.5D	: 2.5 Dimensional
2D	: 2 Dimensional
3D	: 3 Dimensional
BSA	: Bovine Serum Albumin
DAPI	: 4′,6-diamidino-2-phenylindole
DMEM	: Dulbecco's Modified Eagle Medium
DMSO	: Dimethyl Sulfoxide
ECM	: Extracellular Matrix
FBS	: Fetal Bovine Serum
FDA	: Food and Drug Administration
GBM	: Glioblastoma Multiforme
IC50	: Half-Maximal Inhibitory Concentration
MTT	: 3-(4,5-Dimethylthiazol-2-yl)-2,5-Diphenyltetrazolium Bromide
PBS	: Phosphate-buffered Saline
SEM	: Scanning Electron Microscopy
TCPS	: Polystyrene Tissue Culture
TFP	: Trifluoperazine
UPW	: Ultrapure Water

LIST OF SYMBOLS

µL **:** Microliter

µm **:** Micrometer

µM **:** Micromolar

cm^2 **:** Square centimeter(S)

g **:** Gram

mL **:** Milliliter

mM **:** Milimolar

nm **:** Nanometer

rpm **:** Revolutions per minute

1. INTRODUCTION

Cell culture techniques play a vital and important role in the release of pharmaceutical goods, in the analysis of cancer and in the study of stem cells. Most cells are now perfected using two-dimensional (2D) techniques, but new and sophisticated step-by-step approaches that execute three-dimensional (3D) cell perfected procedures indicate convincing proof that even more detailed research can be conducted. The cell-cell or cell-material environment can be monitored when conducting 3D cell culture experiments to be able to provide more detailed knowledge about cell-to-cell interactions, such as for tumor morphology, drug testing, metabolic profiling, stem cell inquiry [1] .

In vitro cell culture techniques divide into 3 main groups according to the dimension; 2D, 2.5 D and 3D. Traditionally used two-dimensional cell cultures have been used *in vitro* to study biophysical and biochemically incoming cell signals. Although it has been accepted until today, with increasing evidence, it has been shown that cell bioactivity in two-dimensional systems deviates significantly. For example, some important features of cancer cells cannot be properly observed in these systems. To solve these problems, 3D cell culture systems are being developed for better observation and analysis of cancer and normal cell lines *in vivo* [2].

Mammalian cell culture, *in vitro*, offers a defined stage for studying the basic morphology of the living being's cell and tissue, and pathophysiology. This was typically achieved by optimized single-cell communities on two-dimensional (2D) substrates such as polystyrene tissue culture (TCPS) or tissue analog surfaces [3]. This 2D experiment with cell formation, molecular biology, stem cell was the foundation for our study of complex biological processes like differentiation and morphogenesis of the tissue. Furthermore, 2D studies have led to pioneering results in the complex relationship between cell structure and cellular microenvironment interactions [4]. In adherent 2D cultures, cells grow as a single layer in a cultivated flask attached to a plastic surface or in a flat petri dish and since the early 1900s it has been the basic technique which was used for cultivating cells. The benefits of 2D cultures are linked to simple and low-cost cell culture management and functional testing efficiency. In addition, 2D cell culture can be manipulated more easily than 3D cultures, and cell morphology determination, environmental control and cell analysis can be performed more easily. Also, it

is easier to compare results from experiments in the literature because there is a lot of data [5]. However, the main disadvantage of 2D cultures is the absence of 3D cell and material interactions as it is in our body [1], [6]. It is important to simulate *in vivo* like environment for natural normal or tumor tissue structures for decreasing workload in preclinical and clinical studies [7].

Glioblastoma multiforme (GB) is the most severe of gliomas, a group of tumors that occur at intervals from interstitial tissue or their precursors in the central nervous system. It is classified as Grade IV in compliance with the World Health Organization (WHO) [8], [9]. Glioblastoma are highly heterogeneous, and immune to medicines. Development of cell lines that maintain consistency and duplicability in experiments are a critical step to evaluate the key characteristics of GB such as proliferation and invasion [9], [10]. There is a strong demand for GBM cell models which are readily accessible and valid. Several GC lines, including U87 (> 1900 quotes in PubMed), U251 (> 1100 quotes), and T98 G (> 900 quotes), have been commonly used in this sense for 30 years, offering useful information about this form of tumor. For certain factors, however, certain versions are incomplete [11]. The well-known third GB cell line is T98G. The cell line T98G was derived from a 61-year-old human male and has a chromosome count of hyperpentaploid with a modal number ranging from 128 to 132. In mice, the cells are not tumorigenic but proliferate in cell culture with adequate anchorage. T98G cells are known to have high expression of the ACTA2 gene engaged in motility and structure of cells. T98G cells are polyploid forms of the parent T98 cell line and can remain under stationary conditions in the G1 step of the cell cycle [12]. It is usually used in drug screening and experimental molecular GB models. It can represent the most common proliferative and intrusive GB phenotype in ex vivo, *in vitro* and *in vivo* experiments. In particular, T98G intrusive ability of cells from the cell / matrix, a shift from epithelial mesenchymal (EMT) migration and proliferation, as well as metabolic and microenvironmental factors [9], [13], [14].

Trifluoperazine (TFP) is FDA-approved antipsychotic drug which is used as a neuroleptic for treating schizophrenic psychosis and thiodiphenylamine by-product. It inhibits cell proliferation and invasion and is being used to induce death in many kinds of neoplastic cell lines and animal models [15], [16] such as lung cancer [17], breast cancer [18], pancreatic cancer [19], colorectal cancer [20], glioblastoma [16]. Moreover, TFP may inhibit the

proliferation, migration and invasion of glioblastoma cells. A mechanistic analysis showed that TFP's anti-glioblastoma function is regulated by increasing the level of Ca+2 intracellular by opening inositol 1,4,5-trisphosphate receptor (IP3R) subtype 1 and 2 as a result of calmodulin (CaM) subtype 2 dissociation from IP3R. However, *in vivo* TFP-treated brain xenograft mouse model did not demonstrate any improvement in survival time [21].

With this, as stated above, it cannot fully simulate the *in vivo* response to potential drug molecules in 2D cell cultures. In order to create an *in vivo*-like environment with the 2.5-dimensional hydrogel to be developed in the thesis proposal and to reveal the effects of the hydrogel and the potential drug molecule on cells in a realistic way, into 2 different cell culture dimensions and different trifluoperazine concentrations, cell viability and morphology of glioblastoma (T98G) cells were investigated.

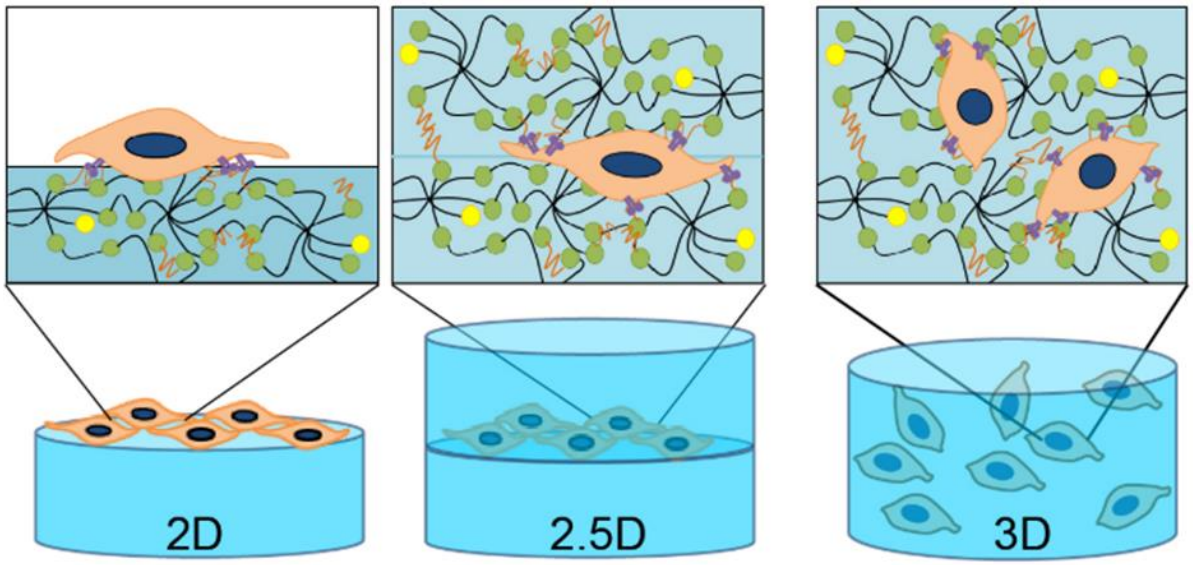

Figure 1.1. Approach for the culture of human pulmonary fibroblasts in 2D, 2.5D, and 3D geometries. Human pulmonary fibroblasts were cultured on top of hydrogels (2D culture), between two hydrogel layers (2.5D culture), or encapsulated within hydrogels (3D culture) [22].

1.1. Aim

In studies examining cancer-drug interactions, it has been shown that 3D culture systems mimic conditions in living organisms better than 2D culture media, and therefore more realistic results are obtained. Accordingly, 2.5D cell culture media are cultures developed to take advantage of 3D cell cultures and reduce their disadvantages. The development of 2.5D cell culture systems increases the accuracy of results by minimizing the artificial polarity that occurs in cells cultured in 2D systems. Glioblastoma is the most common and aggressive malignant primary brain tumor, accounting for more than 50% of all brain tumor cases. T98G cells are a human glioblastoma cell line and are routinely used as experimental models to improve cancer treatment modalities. Treatments with drugs prolong the life expectancy of patients by only about 2.5 months, and tumor recurrence is frequently observed. Therefore, it is very important to develop more effective anticancer treatments for glioblastoma. Trifluoperazine (TFP) is an FDA-approved antipsychotic and antiemetic drug used to treat schizophrenia. It has been shown to inhibit the proliferation and invasion of different cancer cells and induce cell death in various cancer cell lines and animal models.

In the thesis study, the creation and characterization of a 2.5D cell culture system with chitosan-glycerolphosphate-genipin and the 2.5D cell culture system and 2D polystyrene to be developed in the presence and absence of Trifluoperazine (TFP) of the glioblastoma multiform (GBM; Glioblastoma multiforme) cell line T98G glioblastoma cells. In this study, it was aimed to investigate the advantages and disadvantages of the 2.5D cell culture system formed with chitosan-glycerolphosphate-genipin compared to the 2D culture system by aiming to examine the cell viability and morphology comparatively on tissue culture (TCPS; Tissue Culture Polystyrene) surfaces.

2. THEORETICAL FOUNDATIONS AND LITERATURE REVIEW

2.1. Cell Culture

2.1.1. Cell Culture Systems

Literally, dimension is the topological measurement of an object's (or space's) defining attributes (height, width, depth, space-time) symbolizes the state of zero dimensions (non-dimensionality). A line having merely a length measurement is one-dimensional (1D). Two-dimensional (2D) are objects having height and length (square, rectangle, etc). Objects with dimensions of height, width, and depth demonstrate three-dimensionality (3D). The fourth dimension (4D) is time as it is disclosed or felt by the motion of objects in space; time is revealed or felt by the motion of objects in space. Living systems have three-dimensional morphology and anatomy. Since molecules are in motion or vibration, they facilitate the discovery and monitoring of time, the fourth dimension. Living systems are the prototypical example of space-time cohabitation due to the fact that every event in living organisms occurs in time. In light of this, the 4D axis defines and explains vitality, pathology, sickness, and death [23].

In vivo, under the impact of their microenvironment, cells generate polarization in their surrounding environment. Depending on the appropriate amount of polarization [24], the integrity and homeostasis of the tissue, which is a three-dimensional structure, may be maintained. In monolayer cell cultures created *in vitro,* cells elongate and lose their height and depth to a significant degree. Monolayer cell culture is therefore considered a 2D cell culture paradigm. In the *in vitro* 3D cell culture (spheroid) paradigm, however, cells exhibit *in vivo*-like polarization, thus their morphology approaches *in vivo* [25], [26]. In 3D cultivation, cells restore lost depth and variable height and length measurements (Figure 2.1.)

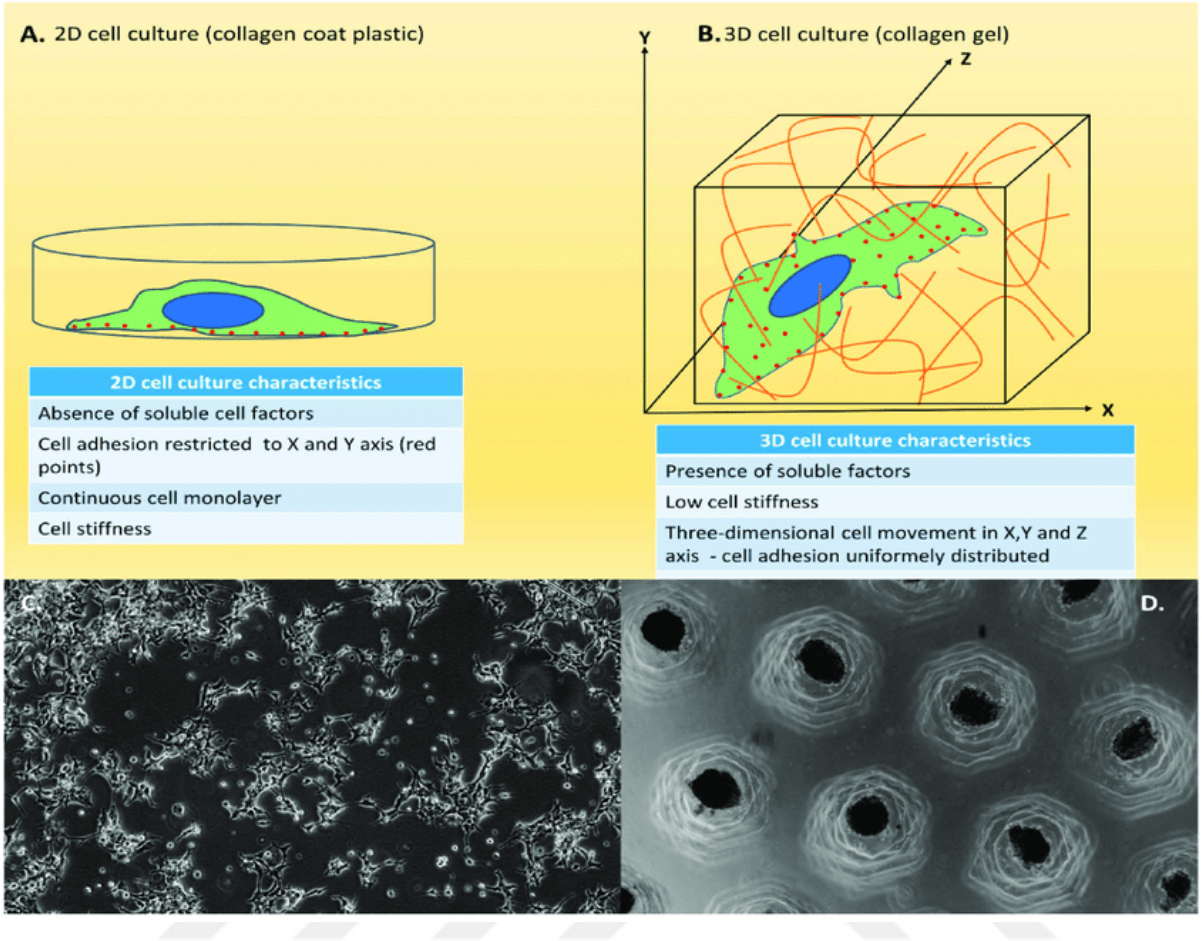

Figure 2.1. Two-dimensional (2D) and three-dimensional (3D) cell culture [27]

2.1.2. 2D &3D Environment

To determine the toxic effect of a molecule (drug, chemical, etc.) on a cell, *in vitro* cell cultures are the first approach employed. Using culture plates, conventional cell cultures offer monolayer and 2D development of anchorage-dependent cells. Due to the rapid generation of large cell populations in this model, the determination of cytotoxicity by cell viability assays is practicable and cost-effective. The containers in which cells are cultivated do not mirror the in-vivo milieu, and the cells are unable to build their *in vivo* microenvironment. This form of cell reproduction leads cells to lose polarity and produce extracellular matrix (ECM) molecules from a restricted location, leading them to lose their *in vivo* characteristics. Although the resemblance of *in vitro* research to *in vivo* and the applicability of their results have been debated for many years, these investigations continue to be significant since they give early data and foresight. Recent technological advancements have made it feasible to cultivate cell lines *in vitro* in three dimensions [3], [4].

3D cell culture is a model system that partially mimics *in vivo* events by allowing cell aggregates to form as tissue spheroids, embedded cells on a scaffold, or liquid-based methods in which structural proteins and other biological molecules found in living tissues mimic the extracellular matrix (ECM). 3D cell culture may be used to regulate cell-cell and cell-matrix interactions, cell proliferation, and differentiation in order to preserve tissue architecture and homeostasis similar to those *in vivo*. Providing an *in vivo*-like milieu in *in vitro* research in which cells may completely produce ECM molecules is crucial for translating *in vitro* results to *in vivo* [28], [29].

The 3D culture models have proved to be a lot more practical to interpret the study results for *in vivo* applications, while cell lines offer us glorious reliable study content, cultivating them as 3D models induces them to act in a way that is a bit closer to nature. To date the approach to 3D culture has been used to test already 380 cell lines. The extra cellular matrix structure in natural tissue differs according to the cell types so, 3D culture conditions should be specified for every cell type. Matrix stiffness, pore structure, pore dimension, interconnectivity is crucial to provide optimal and suitable microenvironment conditions [30], [31]. Appropriate pore diameter is necessary for cell nutrition, proliferation, tissue vascularization, formation of new tissues and migration. Materials with suitable biomechanical conditions such as matrix stiffness, pore dimension ensure efficient release of bio-signal molecules in the cell-material construct [30]. Three-dimensional (3D) cell culture systems have seen physiologically more suitable *in vivo* data for testing and predictive drug discovery due to the obvious advantages in data provision and increased interest in tissue engineering. [32]. The studies have found that cells in 3D culture media dissent morphologically and physiologically from cells in 2D culture media [33]–[35]. Subsequently, the advent of 3D culture has seen rapid progress in recent decades, as demonstrated by the growing number of studies in this study area, including preclinical drug screening, maintenance and differentiation of cancer stem cells, signal abnormal transduction. A that number of tumor biologists have therefore begun to stress the importance of the culture of 3D tumor cells. For e.g., cells in 3D culture typically show a reduced susceptibility to certain chemotherapeutic agents relative to 2D monolayer cultures [36]. Additionally, the 3D tissue culture method enables imitation cancer tissue to be produced [6].

For research objectives, scaffolding and liquid-based approaches can be chosen to construct a three-dimensional cell culture. The two categories of scaffold-based approaches are hydrogel and matrix [37]–[39]. Suspended drop, ultra-low adhesion microplates, microcarrier systems, rotation-based systems, and microfluidic chips are the five categories of liquid-based approaches [39]–[42].

Table 2. 1. Comparison of 2D and 3D cell culture methods. [6]

Type of culture	**2D**	**3D**
Time of culture formation	Within minutes to a few hours	From a few hours to a few days
Culture quality	High performance, reproducibility, long-term culture, easy to interpret, simplicity of culture	Worse performance and reproducibility, difficult to interpret, cultures more difficult to carry out
In vivo imitation	Do not mimic the natural structure of the tissue or tumor mass	In vivo tissues and organs are in 3D form
Cells interactions	Deprived of cell-cell and cell-extracellular environment interactions, no *in vivo*-like microenvironment and no "niches"	Proper interactions of cell-cell and cell-extracellular environment, environmental "niches" are created
Characteristics of cells	Changed morphology and way of divisions; loss of diverse phenotype and polarity	Preserved morphology and way of divisions, diverse phenotype and polarity
Access to essential compounds	Unlimited access to oxygen, nutrients, metabolites and signaling molecules (in contrast to *in vivo*)	Variable access to oxygen, nutrients, metabolites and signaling molecules (same as *in vivo*)
Molecular mechanisms	Changes in gene expression, mRNA splicing, topology and biochemistry of cells	Expression of genes, splicing, topology and biochemistry of cells as *in vivo*
Cost of maintaining a culture	Cheap, commercially available tests and the media	More expensive, more time-consuming, fewer commercially available tests

2.2. 2.5D Cell Culture

2.5D cell culture (pseudo 3D) studies are performed. 2.5D cell culture mimics the 3D structure. For example, the result of an experiment to understand how cell migration occurs in 2.5D cultures has shown the powerful role of matrix structure in regulating cell migration [43]. In another article, it was aimed to enable optical microscopy characterization by applying a new 2.5D scaffold approach. In this article, they presented a 2.5D approach that mimics the processing conditions of 3D salt-washed scaffolds. For the 2.5D approach, the salt-leached technique was used and the PCL-PDLLA (poly-dl-lactic acid and polycaprolactone) blend films were coated with NaCl crystals before annealing, to show that the presence of NaCl strongly influences the polymer mixture surface morphology and cell adhesion, mimicking the 3D scaffold with AFM and light microscopy scaffolding. They presented the 2.5D approach that provides surface properties. During cell culture in 2.5D structures, osteo-blast (MC3T3-E1) and dermal endothelial cell (MDEC) cells were used and chondrogenic cell (ATDC5) adhesion was decreased in NaCl-annealed PCL-PDLLA blends while their adhesion was increased [44].

In another study, it was observed that the resulting 2.5D structures provide a restricted 3D environment for nerve growth. Using a digital micro mirror system (DMD) the technique used in this study has been adapted to create dynamic photo masks to crosslink geometrically specific poly- (ethylene glycol) (PEG) hydrogels induced by free radical polymerization initiated by UV. The resulting "2.5D" structures provide nerve growth with a restrained 3D environment. They used a dual hydrogel approach in which the PEG acts as a site of cell restriction providing structure for an amorphous but cell-permitting self-assembly gel made from Puramatrix or agarose. The process is a quick and simple phase processing, which is highly reproducible and easily adapted for use with traditional methods and substrates for cell culture [45]. 2.5D cultures are used in drug screening. The potential use of 99 FDA approved drugs was investigated *in vitro* on a 2.5D model to understand the behavioral characteristics and drug responses of Pancreatic ductal adenocarcinoma (PDAC) cells [46]. Also, 2.5D organoids have been observed to have a similar sensitivity profile to parental 3D organoids for anti-cancer drug therapy [47].

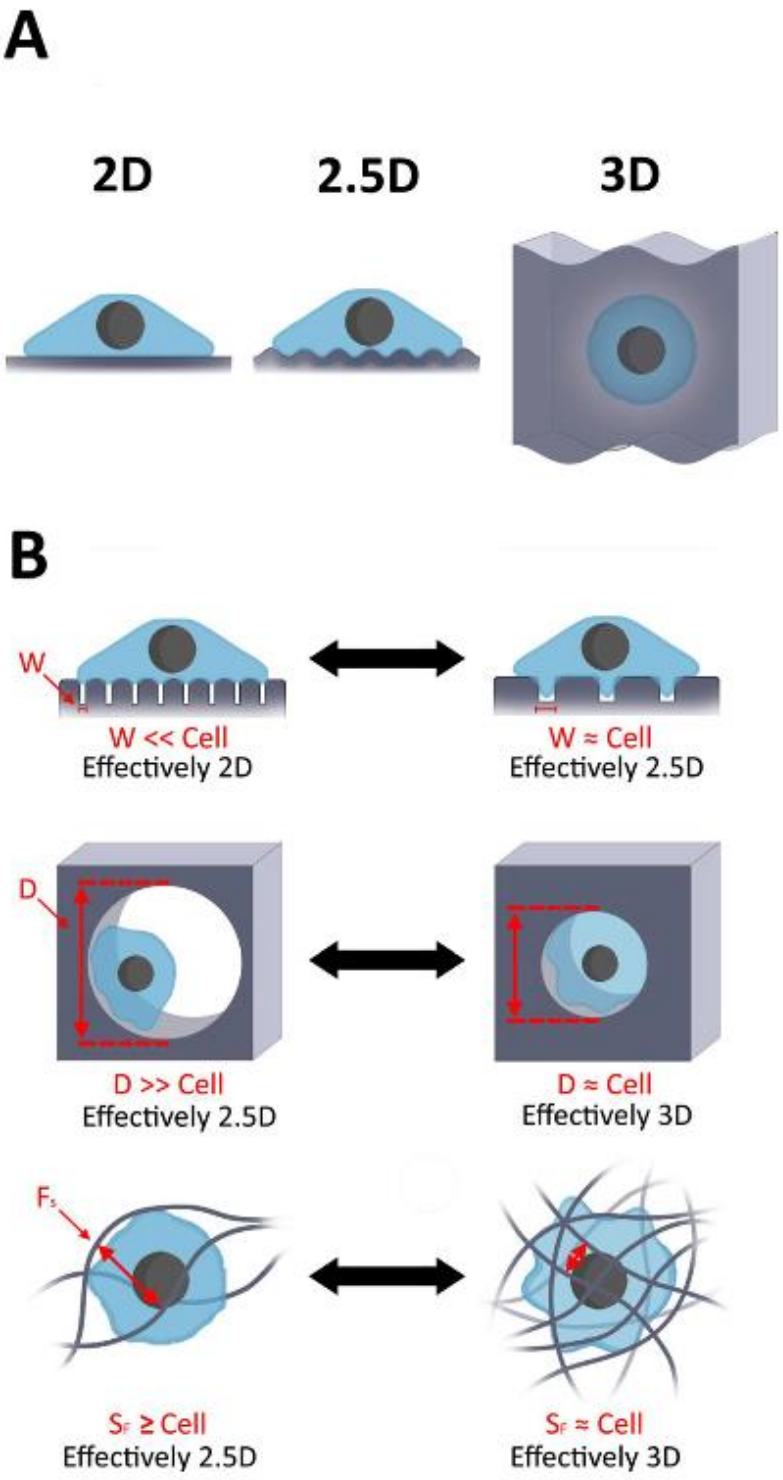

Figure 2.2. Classification and ambiguity of 2D, so-called 2.5D, and 3D culture systems [48].

2.3. Glioblastoma

Constant connection between glial cells and neurons allows them to control neuronal metabolism and interneuron signaling. Astrocytes, oligodendrocytes, microglia, and ependymal cells are the four major subtypes. Gliomas are the common name for tumors that develop from these cells. About 80% of all tumors in the brain are gliomas, which develop from glial cells. It occurs at a rate of 7 cases per 100,000 people over the world [49], [50].

Gliomas are categorized based on the cell type from which they originate: astrocytoma, oligodendroglioma, ependymoma, and mixed glioma. WHO categorized astrocytomas into four subtypes: Stage I or pilocytic astrocytoma, Stage II or low stage astrocytoma (AGII), Stage III or anaplastic astrocytoma (AGIII), and Stage IV or glioblastoma (GBM, Glioblastoma multiforme). GBM is the most lethal kind of glioma, occurring in 65% of cases. It is reported that men over the age of 40 are primarily affected. The treatment of GBM patients includes surgery, radiation, and chemotherapy. GBM patients live between 12 and 15 months and have a 5% 5-year survival rate. Diffuse infiltration of GBM cells into the normal brain parenchyma, persistent tumor development, and tumor cell resistance to radiation and chemotherapeutics are factors that delay and complicate therapy [49].

There is a strong demand for GBM cell models which are readily accessible and valid. Several GC lines, including U87 (> 1900 quotes in PubMed), U251 (> 1100 quotes), and T98 G (> 900 quotes), have been commonly used in this sense for 30 years, offering useful information about this form of tumor. For certain factors, however, certain versions are incomplete [51]. The well-known third GB cell line is T98 G. The cell line T98 G was derived from a 61-year-old human male and has a chromosome count of hyperpentaploid with a modal number ranging from 128 to 132. In mice, the cells are not tumorigenic but proliferate in cell culture with adequate anchorage. T98 G cells are known to have high expression of the ACTA2 gene engaged in motility and structure of cells. T98 G cells are polyploid forms of the parent T98 cell line and can remain under stationary conditions in the G1 step of the cell cycle [12]. It is usually used in drug screening and experimental molecular GB models. It can represent the most common proliferative and intrusive GB phenotype in ex vivo, *in vitro* and *in vivo* experiments. In particular, T98G intrusive ability of cells from the cell / matrix, a shift from epithelial mesenchymal (EMT) migration and proliferation, as well as metabolic and microenvironmental factors [9], [13], [14].

2.3.1. Glioblastoma Microenvironment

It has been revealed that ECM molecules in the brain, specifically hyaluronan, play a significant role in glioma cell invasion and malignancy. The lack of an *in vitro* model in which matrix systems including the compositional and structural aspects of the glioma community surrounding the brain tissue may be produced *in vivo* [52] is the greatest barrier to understanding the extracellular impacts of GBM invasion. Three-dimensional (3D) cell culture may be the best option for simulating GBM, as it resembles *in vivo* in this regard. 15 to 25 percent of typical brain tissue contains extracellular space. The remaining components of the brain include neurons, glia, astrocytic processes, and blood vessels. Neurons and glia produce many ions, neurohormones, peptides, metabolites, and ECM components into the extracellular environment. Non-protein-bound hyaluronic acid and sulfated glycosaminoglycans, such as protein-bound heparan sulfate and chondroitin sulfate, are found in the brain extracellular matrix (ECM). It also includes collagen, laminin, and fibronectin, which contribute to the formation of blood vessels [53].

The microenvironment has a crucial influence on GBM development. All glioma cells, including GBMs, produce ECM components (hyaluronic acid, fibronectin, laminin, collagen, vitronectin, tenascin, etc.), enzymes, and matrix metalloproteinases in their surroundings to assist invasion and alter the ECM in regions of active invasion. In brain tissue, hyaluronic acid is the most significant (main) ECM molecule. Glioma development is defined by variations in the amount of hyaluronic acid molecules in the environment. GBMs express significantly greater amounts of hyaluronic acid than normal brain tissue. GBM cells are able to develop the ideal milieu for migration, proliferation, and invasion when there is an excessive concentration of hyaluronic acid within the cell. Accumulation of extracellular hyaluronic acid is related with intracellular signaling pathways that govern GBM growth and motility [52]. In this aspect, *in vitro* GBM studies do not create an *in vivo*-like microenvironment by secreting ECM molecules from limited surfaces as a result of cells sticking to culture dishes with particular surfaces in standard 2D cell culture. This results in the differentiation of intracellular signaling pathway activation according to *in vivo* settings. In 3D cell culture, on the other hand, activation of signal pathways is comparable to *in vivo*, as cells may form a spheroid structure without adhering to a hard surface such as a culture plate, and ECM molecules can concentrate around them and proliferate in an *in vivo*-like microenvironment [49], [52], [53].

2.4. Drug Repurposing

2.4.1. Drug Repurposing for Cancer Therapy

Drug repositioning is an approach to identify new uses of drugs outside the scope of their original medical indications. In this approach, drugs/compounds that are approved, withdrawn, archived, or undergoing clinical phase studies are identified for uses other than their previously defined targets and their potential to be used for the treatment of other diseases is investigated. Toxicity, efficacy, pharmacokinetics, and pharmacodynamics need to be thoroughly tested, in addition to being designed and manufactured. Most drugs that pass Phase I trials are not approved by FDA. Perhaps the greatest advantage of repurposing a drug is that it is already FDA approved. [54].

The ability to move directly into clinical trials has made this technique widely used in the development of cancer treatments. Thalidomide is one of the most common examples of drug reuse in cancer treatment. Thalidomide has been used as a sedative to this day. It is then used to reduce morning sickness in pregnant women. The drug caused serious birth defects. For this reason, it was withdrawn from the market in 1961. It is one of the main chemotherapy drugs used in GBM treatment today. [54] .

This study investigated the anti-cancer effects of trifluoperazine, an agent approved by the FDA for the treatment of schizophrenia, on the GBM cell line T98G in two- and two-and-a-half dimensional cell culture systems in genipin and crosslinked chitosan hydrogel. Cost, availability in pure form, and novelty are the three main factors involved in drug repurposing. Trifluoperazine is a low-cost drug that is available as a pure molecule from a number of different suppliers.

Table 2.2. Original and new anticancer indications of repurposed drugs [54] .

DRUG	Original indication	New anticancer indication
Thalidomide	Antiemetic in pregnancy	Multiple myeloma
Aspirin	Analgesic, antipyretic	Colorectal cancer
Valproic acid	Antiepileptic	Leukemia, solid tumors
Celecoxib	Osteoarthritis, rheumatoid arthritis	Colorectal cancer, lung cancer
Statins	Myocardial infarction	Prostate cancer, leukemia
Metformin	Diabetes mellitus	Breast, adenocarcinoma, prostate, colorectal
Rapamycin	Immunosuppressant	Colorectal cancer, lymphoma, leukemia
Methotrexate	Acute leukemia	Osteosarcoma, breast cancer, Hodgkin lymphoma
Zoledronic acid	Anti-bone resorption	Multiple myeloma, prostate cancer, breast cancer
Leflunomide	Rheumatoid arthritis	Prostate cancer
Minocycline	Acne	Ovarian cancer, glioma
Vesnarinone	Cardioprotective	Oral cancer, leukemia, lymphoma
Thiocolchicoside	Muscle relaxant	Leukemia, multiple myeloma
Nitroxoline	Antibiotic	Bladder, breast cancer
Noscapine	Antitussive, antimalarial, analgesic	Multiple cancer types

2.4.2. Typical Antipsychotic

Typical antipsychotics emerged in the 1950s and are widely used in the treatment of various mental illnesses such as schizophrenia, schizoaffective disorder, some types of bipolar disorder and delusional disorders [55] . Based on their chemical structure, FGAs are classified as phenothiazines (e.g., trifluoperazine), butyrophenones, and thioxanthenes. Inhibition of dopamine receptors of the D2 family is their common mechanism of action. Based on their chemical structure, FGAs are classified as phenothiazines, butyrophenones and thioxanthenes. Blocking D2 family dopamine receptors is their common mechanism of action. This blockade of the mesolimbic pathway is probably related to the therapeutic effects of FGAs. [56].

Additionally, mesocortical, nigrostriatal, and tuberoinfundibular pathways are affected by the blockage of dopamine D2 receptors by FGAs. As a result, overdose consumption causes secondary side effects and cognitive impairments, extrapyramidal symptoms, and hyperprolactinemia [57]. In addition, due to their other pharmacological activities, they exhibit additional adverse effects, including sedation, constipation, and cardiovascular issues [56].

In addition to their antipsychotic effects, phenothiazines demonstrate a variety of biological actions that are associated for their possible anticancer activity, including reversal of MDR by downregulation of PGP and inhibition of calmodulin, protein kinase C and cell proliferation. [58]. In a related finding, research on the anti-cancer potential of the phenothiazines has shown that schizophrenia patients have a lower risk of cancer than the general population. These drugs may also help cancer patients with emotional and social problems, like anxiety and sleep problems [59].

2.4.3. Trifluoperazine

Trifluoperazine (TFP) is an antipsychotic drug approved by the FDA for the treatment of schizophrenia. It works by blocking dopamine D2 in the brain, which makes it an antipsychotic agent. It is a derivative of a phenothiazine that contains a piperazine side chain. Its primary activity, however, seems related to the presence of a trifluoromethyl substituent at the 2-position of the phenothiazine. TFP has been shown to inhibit cell proliferation and invasion and to cause death in a variety of neoplastic cell lines and animal models [15],[16], including lung[17], breast[18], pancreatic[19], colon[20], and glioma[16]. In addition, TFP can inhibit the proliferation, migration and invasion of glioblastoma cells.

TFP reduces calmodulin (CaM) activity substantially, besides its effect of blocking the dopamine D2 receptor, the drug. All eukaryotic cells contain CaM, a calcium-binding protein with multiple functions. CaM is involved in signal transduction cascades, cell proliferation, control of cell motility and cell division. Therefore, the antiproliferative and cytotoxic effects of TFP on several cancer cell lines may be explained by its CaM-blocking activity. [60].

Since PGP phosphorylation is controlled by CaM-activated enzymes, inhibiting CaM activity also results in the downregulation of PGP. It might be a chemosensitizer because it reduces resistance to multiple drugs and makes cells more sensitive to chemotherapy. A mechanistic analysis showed that TFP's anti-glioblastoma function is regulated by increasing the level of Ca^{+2} intracellular by opening inositol 1,4,5-trisphosphate receptor (IP3R) subtype 1 and 2 as a result of calmodulin (CaM) subtype 2 dissociation from IP3R. However, *in vivo* TFP-treated brain xenograft mouse model did not demonstrate any improvement in survival time [21].

2.4.4. Previous Studies on Anti-Cancer Activities of Trifluoperazine

A large number of in vitro and in vivo studies have demonstrated the anticancer effects of TFP in various cancers, including leukemia, lymphoma, breast cancer, lung cancer, melanoma, prostate cancer, and pancreatic cancer [61]-[63].

In 1983, Wei and colleagues demonstrated that TFP could inhibit the growth of a breast cancer cell line. The IC50 of TFP was determined to be 18 M for continuous exposure and 50 M for 1 h exposure [64].

In 1986, Smith and colleagues investigated the effect of hyperthermia and TFP on chromatin structure and DNA damage induced by belomycin (BLM) in the EMT-6 breast cancer cell line. They had previously shown that treatment of EMT-6 cells with both HT and TFP increased the cytotoxicity of BLM. These studies showed that the interaction of DNA with its protein matrix is significantly altered. Therefore, it was hypothesized that the increased cytotoxicity of BLM-treated cells is related to the lethal DNA damage caused by the absence of DNA repair mechanisms in cells treated with HT and TFPs. By demonstrating the potential of chromatin/DNA repair modifying strategies to overcome drug resistance in cancer cells, this work provided a rationale for the use of TFPs in thermochemotherapy [65].

In 1988, Ganapathi and colleagues used male C57BL/6NCr mice that had received DOX and 5M TFP to show that the in vivo effect of doxorubicin (DOX) was enhanced in mice that had received DOX and 5M TFP. Although DOX-TFP was much more effective than DOX alone, there was no correlation between cellular DOX levels and level of resistance after combination therapy. Therefore, they concluded that the effect of TFP on modulating DOX resistance was probably related to molecular changes in the cell rather than to effects on accumulating or retaining the drug[66].

Hait et al. completed a phase I study of bleomycin and TFP combination therapy in 1989. There were no hematologic side effects. The main toxicities were respiratory and neurological. Two of the nineteen patients had partial responses to treatment, while two had complete responses. Hait and coworkers found that TFP can be safely administered with bleomycin at a dose of 9 mg BID [67].

Budd et al. completed a phase II trial of DOX plus TFP in metastatic breast cancer in 1993. The effect of the combination of DOX and TFP was not significantly different from the effect of DOX alone [68].

The effect of serum concentration on the efficacy of several chemosensitizers, including TFP, to reverse PGP-associated MDR was investigated by Lehnert et al. in 1996. Cells were treated with DOX alone and in combination with these chemosensitizers. According to the results, physiological serum protein concentrations reduced the MDR-reversing effect of TFP and some other chemosensitizers [69].

In 1999, Pan et al. showed that human bile duct carcinoma cells treated independently with tamoxifen (TMX) and TFP undergo an induction of apoptosis. Fas antigen is heterogeneously expressed on the surface of human cholangiocarcinoma cells. They used this information to identify and grow Fas-positive and -negative cells. When cells were treated with TMX, TFP, and Fas antibody, only Fas-positive cells were induced to undergo apoptosis [70].

In 2004, Shin et al. investigated the effects of TFP-induced growth inhibition on human U87MG glioma cells. They found that TFP had antiproliferative effects by upregulating the tumor suppressor gene Egr-1, which is involved in cell proliferation, differentiation, and death [71].

In 2009, Chen et al. investigated TFP's anti-cancer effect on the human lung A549 cell line. By inducing apoptosis, they demonstrated that TFP suppressed cell proliferation in a dose- and time-dependent manner [15].

In 2012, Yeh and colleagues demonstrated that TFP inhibited cancer stem cell production and decreased cancer stem cell marker expression in multiple NSCLCs. TFP blocked the Wnt/b-catenin pathway in lung cancer spheroids that were resistant to gefitinib. Moreover, when combined with gefitinib or cisplatin, it had a synergistic effect. In lung cancer mouse models, its inhibitory effect on tumor development was also shown [72].

In 2014, Gross and colleagues showed that TFP has anti-metastatic effects on human prostate cancer cell lines PC3 and C4-2b. They showed that TFP decreased the angiogenic and invasive capacity of aggressive cancer cells, suggesting that TFP may have potential as an anti-metastatic drug for the treatment of prostate cancer [73].

In 2015, Yuan et al. demonstrated an increase in TRA-8-induced apoptosis in TRA-8-resistant pancreatic cancer cells treated with the CaM antagonist TFP. This study proposes the use of these CaM antagonists in combination with TRAIL-activating drugs for the treatment of pancreatic cancer [74].

In vitro and in vivo activation of TFP-treated triple negative breast cancer (TNBC) cells was demonstrated by Park et al. in 2016. They reduced the expression of oncogenes that underlie the emergence of cancer stem cell-like populations in multiple cancers [75].

3. METHODOLOGY

3.1. Materials

In the thesis study, GBM cell line (T98G, (ECACC 92090213)), media of cell cultures (DMEM/F12 w/o hepes, DMEM/F12), Fetal Bovine Serum (FBS), antibiotics (penicillin/streptomycin) used in the preparation of the medium were used. Sterile flasks (25 cm^2 and 75 cm^2) for culturing and multiplying cells, Trypsin/EDTA solution, sterile pipettes with volumes of 5 ml and 10 ml, pipette tips in volumes of 10- 200- 1000 μL, for centrifugation of cells 1.5, 2, 15 and 50-ml volume tubes, cell count slides for cell counting, sterile cryo tubes were used for cell freezing. MTT analysis, Resazurin analysis, and DAPI staining were performed for cytotoxicity and viability tests. In the production of hydrogels, Chitosan which is the main material, acetic acid to dissolve chitosan, Genipin as a cross-linker, and glycerolphosphate to provide acid-base balance were used. Production of hydrogels and seeding of cells was done in a sterile 24-well plate. For viability analysis results, readings were taken on a microplate reader using sterile 96 well plates.

Cell culture processes were carried out in a sterile cabinet, and the working surface was wiped with 70% alcohol after sterilizing the environment with an ultraviolet lamp for at least 15 minutes before each study.

3.2. 2D Culture of T98G Cell line on Tissue Culture Polystyrene

In the first part of the thesis, it was aimed to determine the effect of TFP on T98G cells on TCPS as 2D culture system. Viability of T98G cells in the presence of different concentrations of TFP was determined by MTT analysis, resazurin application and DAPI staining. IC50 value of TFP on T98G cells was calculated from the MTT analysis results. Flow chart of 2D cell culture studies is given in Figure 3. 1 below.

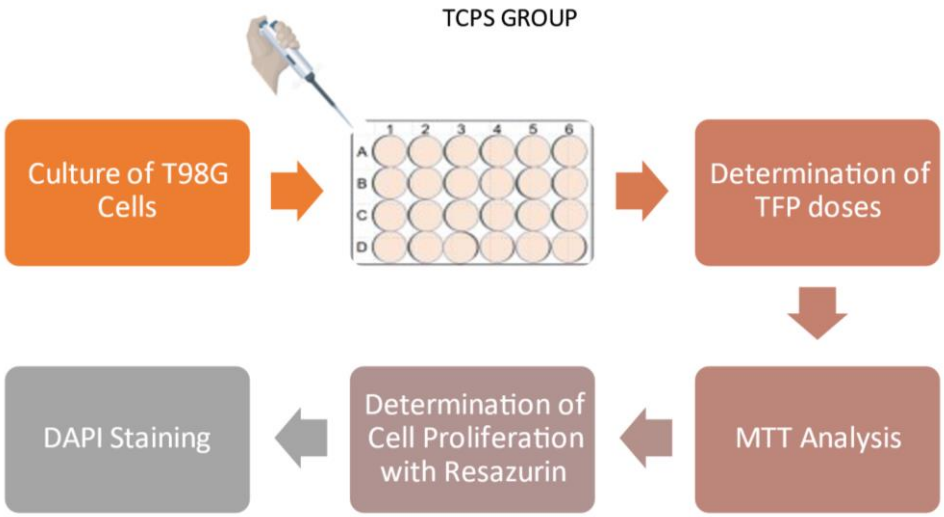

Figure 3. 1. Graphical representation of the studies on TCPS as 2D culture system.

3.2.1. Culture of T98G Cells

Cell culture experiments were performed with the Human Glioblastoma Multiforme Cell Line (T98G, (ECACC 92090213)). After the cells in the liquid nitrogen tank at -196 °C were removed from the tank and thawed at room temperature, Dulbecco's Modified Eagle's Medium-F12 (DMEM-F12) containing 10% Fetal Bovine Serum (FBS) and 1% Penicillin-Streptomycin solution was placed in a sterile 15 mL centrifuge tube. F12) was transferred into the medium and centrifuged at 1000 rpm (rpm) for 5 minutes at 4 °C. After the supernatant was removed at the end of centrifugation, the cells remaining at the bottom were planted in 75 cm^2 culture dishes containing 12 mL of medium and multiplied in an incubator at 37 °C, 5% CO_2 and 95% humidity. The medium was changed every two days and this process was continued until the cells covered 70% of the culture dishes.

3.2.2. Passaging of Cells

After removing the medium in a 75 cm^2 culture dish with a pipette, the cells were washed twice with 5 mL of Dulbecco's Phosphate Buffered Saline (DPBS). Then, in order to remove the cells adhered to the base, 4 mL of 0.25% Trypsin-EDTA solution was placed in culture vessels and removed to the incubator. At the end of a waiting period of about 5 minutes, the cells were checked under the microscope and then transferred to a centrifuge tube containing 9 mL of medium and centrifuged at 1000 rpm for 5 minutes at 4 °C. After the entire supernatant was poured, 1 mL of medium was added, and the cells at the bottom were homogenized with the

help of a pipette, placed in a 75 cm^2 culture dish containing 12 mL of medium and removed to the incubator for proliferation. Cells in culture dishes were monitored daily for viability, proliferation and contamination using an inverted light microscope. The medium of the cells was changed every two days.

3.2.3. Cell Seeding

After the viable cell count was done, $4.8x10^3$ cells in 200 µL volume were inoculated in each well of the 96-well culture dish, and $3x10^4$ cells in 1 mL volume in each well of the 24-well culture dish. After a 24-hour incubation period in incubator, the cells were spread on the TCPS surface and used for the experiments.

3.2.4. Preparation of Drug Dose

Trifluoperazine (TFP) (ChemCruz, sc-201498) was obtained in powder form. It was dissolved in ultrapure water (UPW) and a 2 mM master stock was prepared. Trifluoperazine doses of 1, 2, 4, 6, 8, 10, 20 µM diluted in DMEM-F12 from the stock solution were used in the experiments. The prepared doses were applied to the wells in a volume of 200 µL for 24 and 48 hours. On the other hand, only 200 µL of medium was added to the wells that did not contain the drug and used as a control group. The experiment was designed to have at least 6 wells for each dose.

3.2.5. Determination of Cell Proliferation Based on Mitochondrial Activity (MTT)

The effect of trifluoperazine on cell proliferation was investigated by the 3-[4,5-dimethyltriazol-2-yl]-2,5-diphenyltetrazolium bromide (MTT) assay. 5 mg/mL MTT master stock solution was prepared by dissolving in phosphate buffer saline (PBS) and passing through a 0.22 µm filter. After application of TFP to the cells, 200 µL of 10% MTT in DMEM: F12 was added to each well and incubated for 4 hours at 37 °C, 5% CO_2. At the end of the incubation period, the contents of the culture dish were poured and 200 µL of isopropyl alcohol containing 0.4 M HCl was added to each well to dissolve the formazan salts formed in the living cells. Absorbance values were recorded by a spectrophotometer (BMG Labtech, SPECTROstar Nano, Germany) at a wavelength of 570-690 nm. 690 nm is reference wavelength. Since formazan, the product of MTT, correlated with the number of viable cells, the optical density read in the drug-treated wells was converted to the percentage of viable cells relative to the control. The following formula was used for this process.

$$\text{Cell viability (\%)} = \frac{\text{Absorbance of TFP treated cells in each well x100}}{\text{Average absorbance of control cells}}$$

The dose that caused 50% cell death compared to the control was calculated and accepted as the IC_{50} value.

3.2.6. Determination of Cell Proliferation with Resazurin

As a common indication of cell viability in numerous studies to gauge the biocompatibility of medical materials, resazurin dye has been utilized extensively. The transfer of electrons from NADPH+ H+ to resorufin decreased resazurin is carried out by mitochondrial enzymes acting as carriers of diaphorase activity [61]. The level of reduction was quantified by spectrophotometers since resazurin exhibits an absorption peak at 600 μm and resorufin at 570 μm wavelengths.

0.2 mg/ml resazurin is dissolved in PBS with Ca & Mg. Then the resazurin solution filter-sterilize through a 0.2 μm filter into a sterile, light protected container. Stored at +4 ℃ for up to 2 weeks. The prepared resazurin was diluted at a ratio of 1/10 in the serum cell culture medium and 600 μL was added to each 24-well plate well. It was incubated at 37 ℃ for 2 hours in the dark. Resazurin analysis was compared on both hydrogels and TCPS group.

3.2.7. Immunofluorescent Staining ((4', 6-diamidino-2-phenylindole) DAPI Staining)

Immunofluorescence staining was performed to see the effect of TFP on the nuclear morphology of T98G cells. After the treatment of the cells, the cells were washed 2 times with PBS, then 30 μL of 4% formaldehyde (w/v in PBS) was applied to each well and fixed for 20 minutes. At the end of the period, they were washed 3 times with PBS (PBS/A) containing 1% w/v bovine serum albumin. 30 μL of 0.1% Triton X-100 (in PBS/A) was applied to each well and incubated for 10 minutes. After permeability of the cell membrane, it was washed 2 times with PBS/A. DAPI was diluted with 1/1000 dilution in PBS/A and 40 μl was applied to each well and kept in the dark at room temperature (RT) for 60-90 minutes. After the incubation period, the cells were washed 3 times with PBS/A. The morphologies of the cell nuclei were examined under inverted phase contrast microscope with fluorescence attachment.

3.3. Studies on 2.5D Chitosan Hydrogels

In the second part of the thesis, chitosan, glycerol phosphate, genipin hydrogels were produced and used directly for 2.5D cell culture studies. Surface properties of the hydrogels were determined by SEM analysis. The produced hydrogels were 2.5D and T98G cells were seeded on them. TFP concentrations determined in TCPS group were tested on hydrogels. Cell viability on hydrogels was measured with resazurin. DAPI staining was performed to image the cell nuclei on the hydrogels.

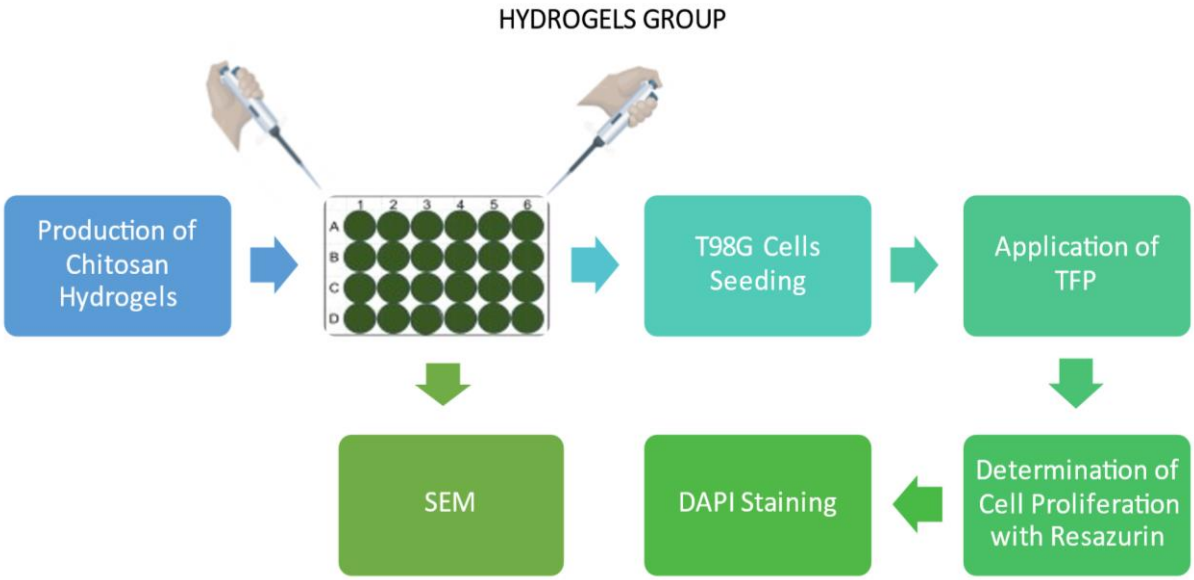

Figure 3. 2. Graphical representation of the studies on Hydrogels as 2.5 D culture system.

3.3.1. Production of Chitosan Hydrogels

For the synthesis of chitosan-based hydrogels, 2 g of chitosan was dissolved in 100 ml of UPW containing 1% (v/v) acetic acid for about one day with magnetic stirrer at RT. The chitosan solution was centrifuged at 5000 rpm for 10 minutes to separate the impurities. It was then passed through a 0.45 µm filter to be taken into the cell culture. The hydrogels were pH-equilibrated with glycerol phosphate (in 1 g/ 1 mL UPW) before cross-linking. During the production of the hydrogels, genipin was applied at different concentrations (1-1.5 mM) for the cross-linking of chitosan and their gelation was examined. Chitosan solution was poured onto the wells of 24 well plate as 200 µL per well. The plates were closed and parafilm coated to

prevent of the drying of the hydrogels. They were then placed in 5% CO_2 incubator for 3 h for gelation. After the gelation completed, excess (unreacted) crosslinker in the hydrogels were washed with culture medium and 500 µL of culture medium was added onto the hydrogels and conditioned in the 5% CO_2 incubator for one day. DMEM-F12 and DMEM-High glucose culture media both were used in the studies to condition the hydrogels.

3.3.2. SEM (Scanning Electron Microscope) Analysis

Scanning electron microscopy (FEI, Quanta 650 Field Emission SEM) was used to determine the morphology of the scaffolds. To prepare hydrogels for SEM analyses hydrogels were made in two groups. First group, 0.5% acetic acid, 1 mM genipin and 5 mL glycerolphosphate (per 5 mL 2% (w/v) chitosan) in 24 wells were frozen at -80 ℃ after gelation. This group is the group used in the experiments. The second group was frozen at -80 ℃ after pouring the hydrogels with the same content into a 5 mL syringe. Hydrogels dried by freeze-dryer. They were cut into 1 mm thick. To provide electrical conductivity, the surface of the tissue scaffolds was coated with gold-palladium, and SEM images were obtained. SEM images were obtained at 250, 500, and 1000x magnifications.

3.3.3. Culture of T98G Cells on The Hydrogels

Hydrogels conditioned in cell media for 1 day in the incubator are aspirated with a cut pipette tip prior to cell seeding. After washing once with PBS medium, 500 µL of medium is placed on it and incubated for 1 more hour. If there is no change in the color of the medium at the end of the period, the cell seeding process is started on the hydrogels. 500 µL of $3x10^4$ T98G in each well of the 24-well cell culture plate is gently dropped onto the hydrogel with a cut-tip pipette. The hydrogels incubated for 1 day at 37 °C, 5% CO_2 and 95% humidity. At the end of 1 day, the cell medium is aspirated over the hydrogels with cell adhesion under the microscope and the TFP treated cell medium is placed and used for the next analysis.

3.3.4. Determination of Cell Proliferation with Resazurin

0.2 mg/ml resazurin is dissolved in PBS with Ca & Mg. Then the resazurin solution filter-sterilize through a 0.2 µm filter into a sterile, light protected container. Stored at +4 ℃ for up to 2 weeks. The prepared resazurin was diluted at a ratio of 1/10 in the serum cell culture medium and 600 µL was added to each 24-well plate well. It was incubated at 37 ℃ for 2 hours in the dark. Resazurin analysis was compared on both hydrogels and TCPS group.

3.3.5. Immunofluorescent Staining (DAPI Staining) in 2.5D Culture

Immunofluorescence staining was performed to see the effect of TFP on the nuclear morphology of T98G cells onto hydrogels. For DAPI staining applied on hydrogels, DAPI staining was applied at different dilutions. DAPI staining process applied at different times and at different dilutions Figure 3.3. shown. After the treatment of the hydrogels, the hydrogels were washed 2 times with PBS, then 100 µL of 4% formaldehyde (w/v in PBS) was applied to each well and fixed for 1 hour at 37 ℃. At the end of the period, they were washed 3 times with PBS (PBS/A) containing 1% w/v bovine serum albumin. 30 µL of Triton X-100 (in PBS/A) was applied to each well and incubated for different time and dark room. After permeability of the cell membrane, it was washed 2 times with PBS/A. DAPI was diluted with different dilution in PBS/A and 50 µl was applied to each well and kept in the dark at room temperature (RT). After the incubation period, the cells were washed 3 times with PBS/A. The morphologies of the cell nuclei were examined under inverted phase contrast microscope with fluorescence attachment. DAPI tested in the Hydrogel control group was observed in only 1 well at a dilution of only 1/500. Therefore, any dyeing process could not be performed on the medicated hydrogels.

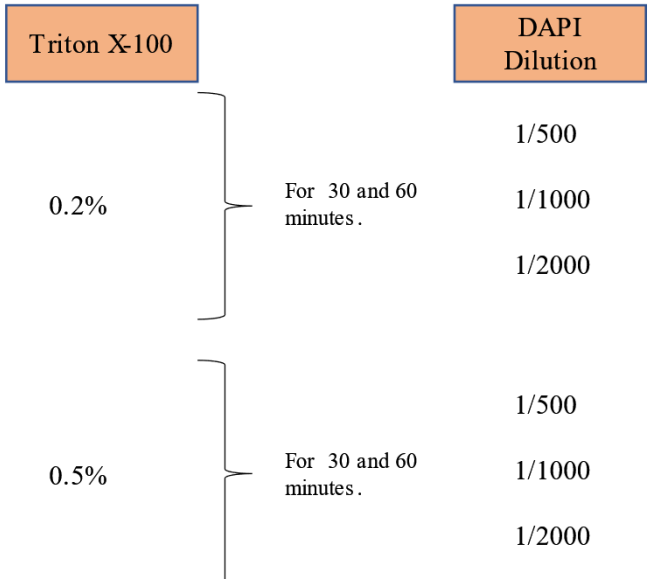

Figure 3. 3. DAPI dilutions applied on hydrogels

4. RESULT AND DISCUSSIONS

4.1. Culture of T98G Cells on TCPS: 2D

The morphological effects of 1, 2, 4, 6, 8, 10 and 20 µM TFP doses on the T98G cell line, depending on the 24- and 48-hour dose and time, were examined with the help of inverted light microscopy and it is given in Figure 4.1.

It was determined that 1 µM dose of TFP tested for 24 and 48 hours did not cause any morphological changes in T98G cells and no difference was observed in terms of cell density compared to control cells. However, it was observed that the normal shuttle-shaped cell morphology disappeared, cells became smaller, intercellular connections and cell number decreased with the decrease in the number of viable cells compared to the control group at 4 µM dose (Figure 4.1 and Figure 4.2).

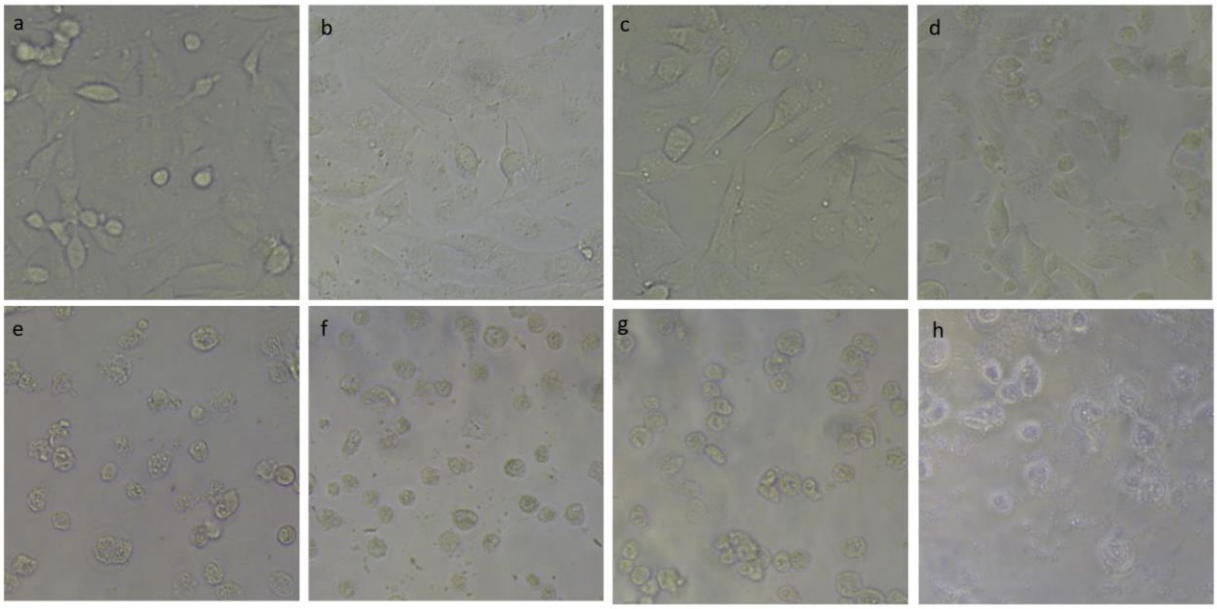

Figure 4.1. Inverted phase contrast images of T98 cells after TFP application for 24 h on TCPS a) Control, b) 1 µM, c) 2 µM, d) 4 µM, e) 6 µM, f) 8 µM, g) 10 µM, h) 20 µM

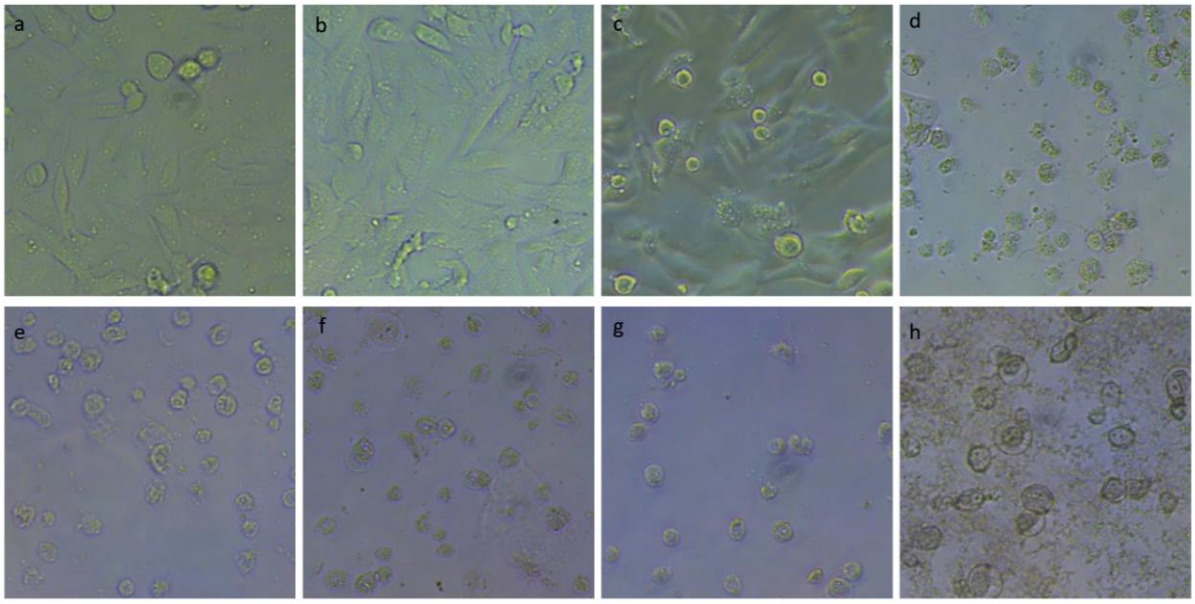

Figure 4.2. Inverted phase contrast images of T98 cells after TFP application for 48 h on TCPS a) Control, b) 1 µM, c) 2 µM, d) 4 µM, e) 6 µM, f) 8 µM, g) 10 µM, h) 20 µM

The impact of TFP on the cellular morphology of T98G cells was examined using cell imaging and analysis. T98G cells were exposed to TFP, and dose-dependent alterations in cellular morphology were seen (1, 2, 4, 6, 8, 10, 20 µM). In reaction to TFP, cell shape changed after 24 hours, the majority of cells fled the plate and died. Furthermore, TFP-treated cells had a considerably lower percentage of growing glioblastoma cells than untreated ones. These findings supported the findings of the MTT experiment, indicating that TFP substantially induces T98G glioblastoma cell death.

4.1.1. Determination of Cell Proliferation Based on Mitochondrial Activity (MTT)

Mitochondrial activity-based MTT method was used to determine the effect of TFP doses on cell proliferation. In the study; TFP doses of 1, 2, 4, 6, 8, 10 and 20 µM were administered on the T98G cell line for 24 and 48 hours. It was determined that 1 µM TFP dose applied for 24 hours did not show a suppressive effect on proliferation in T98G cells. At other doses, cell survival rates of TFP decreased by 98%, 86%, 51%, 3%, 2% and 1% compared to the control. It was determined that 20 µM and 10 µM TFP doses applied for 48 hours completely killed the cells.

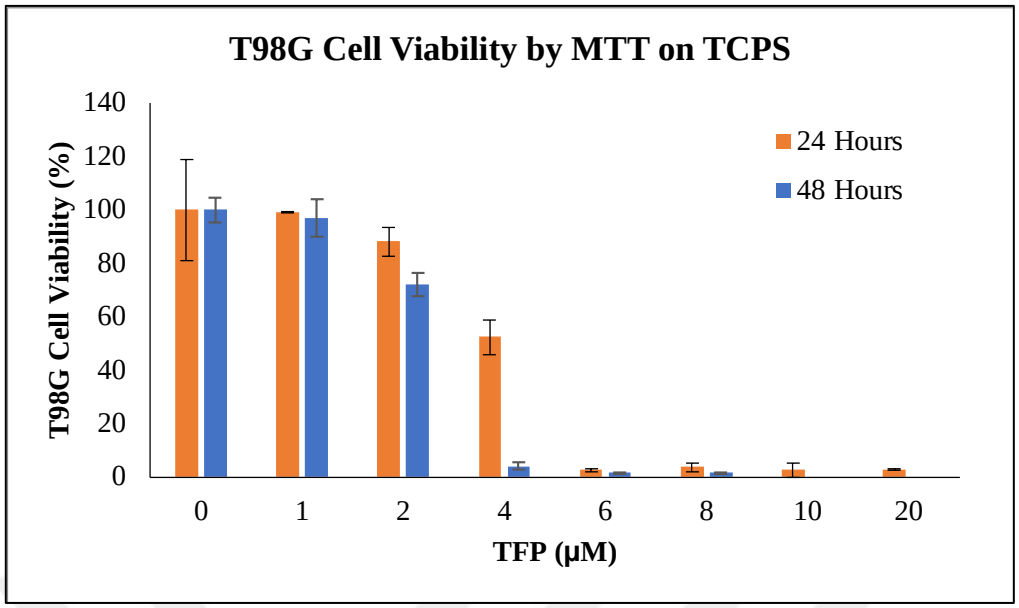

Figure 4.3. Effect of TFP on T98G cell proliferation in a dose- and time-dependent manner on TCPS

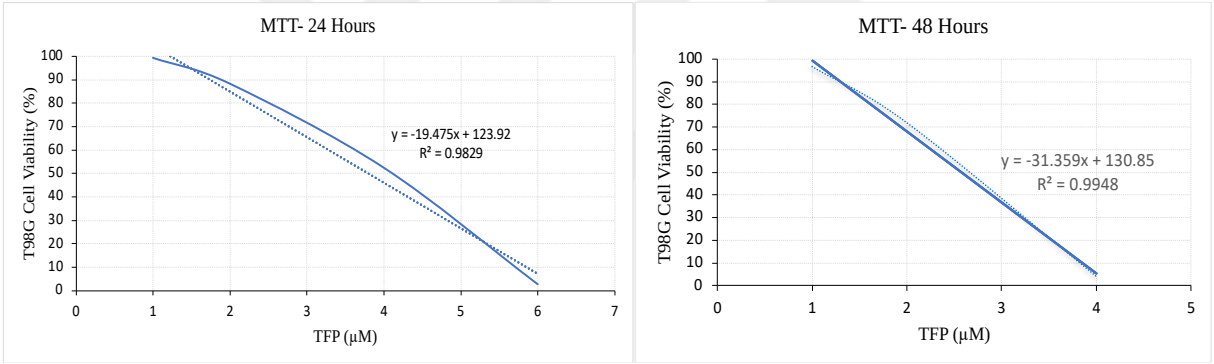

Figure 4.4. The cell viability assay results of (a) 24 hours and (b) 48 hours on TCPS

IC_{50} value, drug dose that causes 50% cell death, expressed as 3.75 µM in 24 hours; IC_{50} of 48 hours was determined as 2.57 µM (Figure 4.4). TFP drug doses were selected as 1 µm, 2 µm, 4 µm, 6 µm and 8 µm were selected to be used in resazurin analysis based on MTT results.

4.1.2. Determination of Cell Proliferation by Resazurin

Resazurin analysis was performed on TCPS at 24 and 48 h. IC50 values were calculated as 2,86 µM at 24 and 2.64 µM at 48 h, respectively (Figure 4.6). Calculated IC50 values were similar to the IC50 values obtained from MTT analysis so, resazurin analysis were selected to be used in hydrogel studies.

TFP was considered a potential reagent for glioblastoma treatment due to its safety and high permeability of the blood-brain barrier [62]. Cell death was observed after 4 µM depending on the TFP concentration within 24 hours. After 48 hours, cells are completely dead after 2 µM TFP concentration in Figure 4.5.

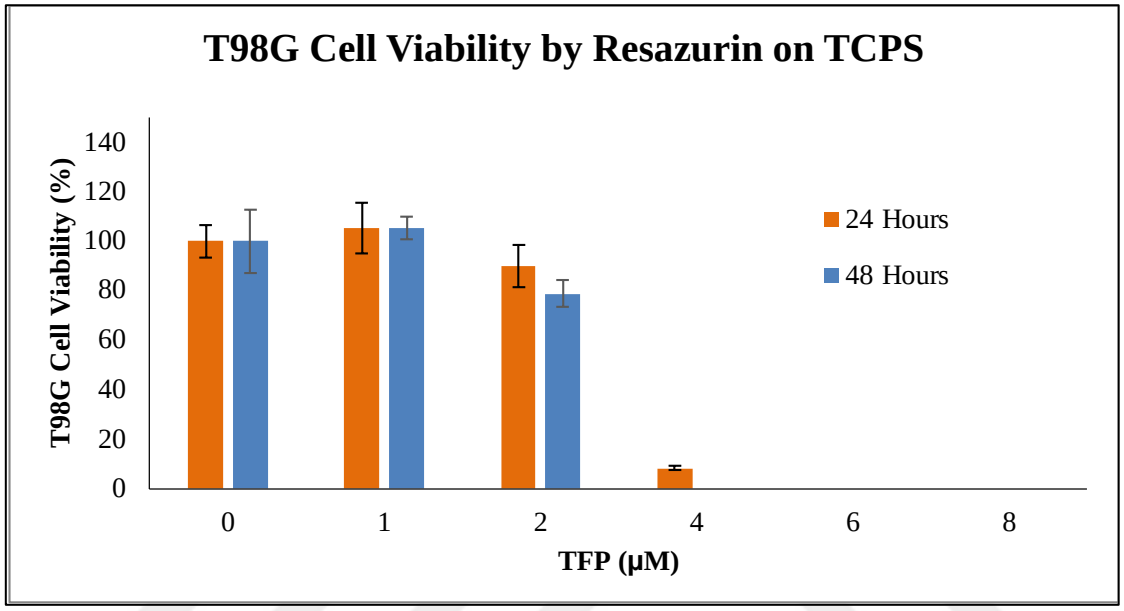

Figure 4.5. Effect of TFP on T98G cell proliferation in a dose- and time-dependent manner on TCPS.

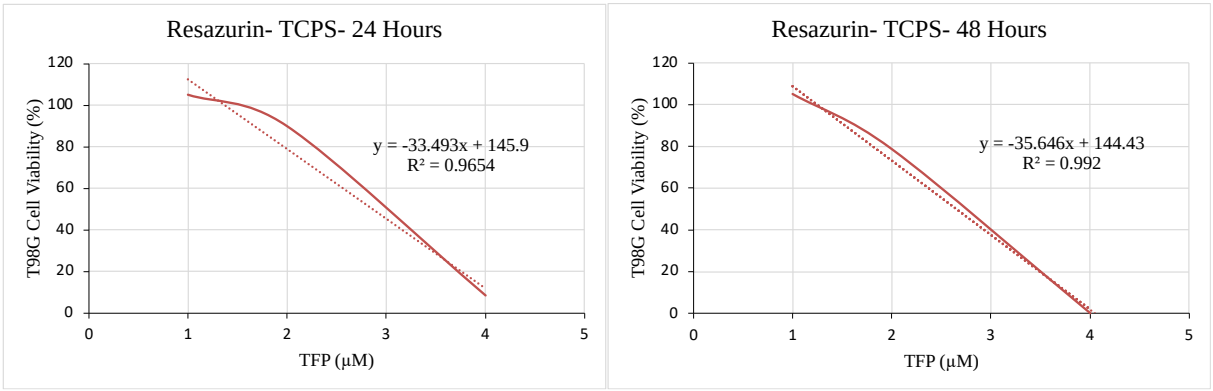

Figure 4. 6. The cell viability assay results of 24 hours and 48 hours on TCPS

On the glioblastoma cell lines U251 and U87, the IC50 values depending on the TFP concentration were 16 and 15 µM, respectively [63]. In another study, the effect of TFP on

U87MG glioblastoma cells was examined at 24 hours and 48 hours, the cytotoxic effect of TFP was observed [62]. The cell viability assay results supported that TFP is also toxic on T98G cells.

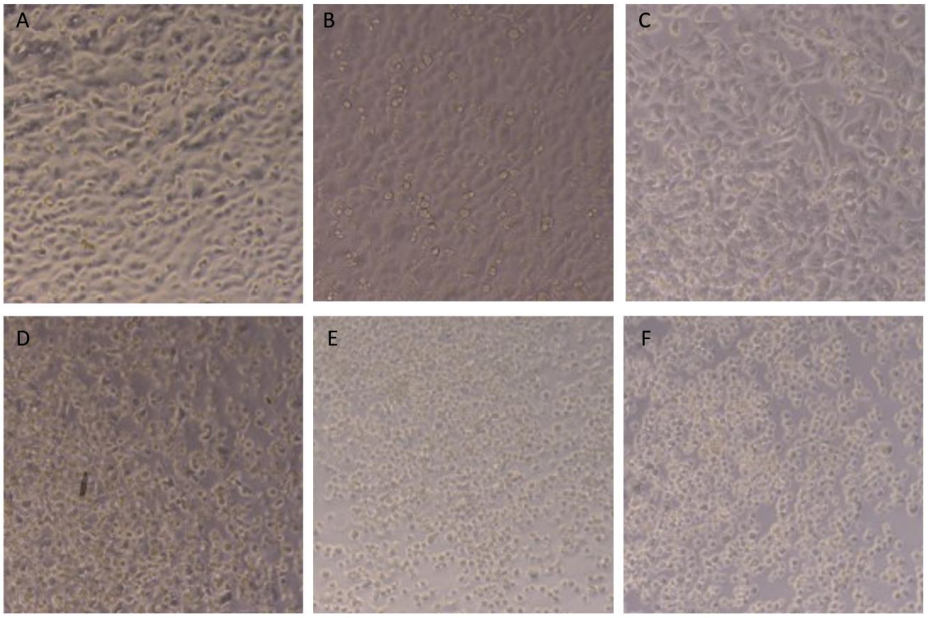

Figure 4. 7. T98G cells on TCPS after 24h culture (10X) a) Control b) 1 µM c) 2 µM d) 4 µM e) 6 µM f) 8 µM.

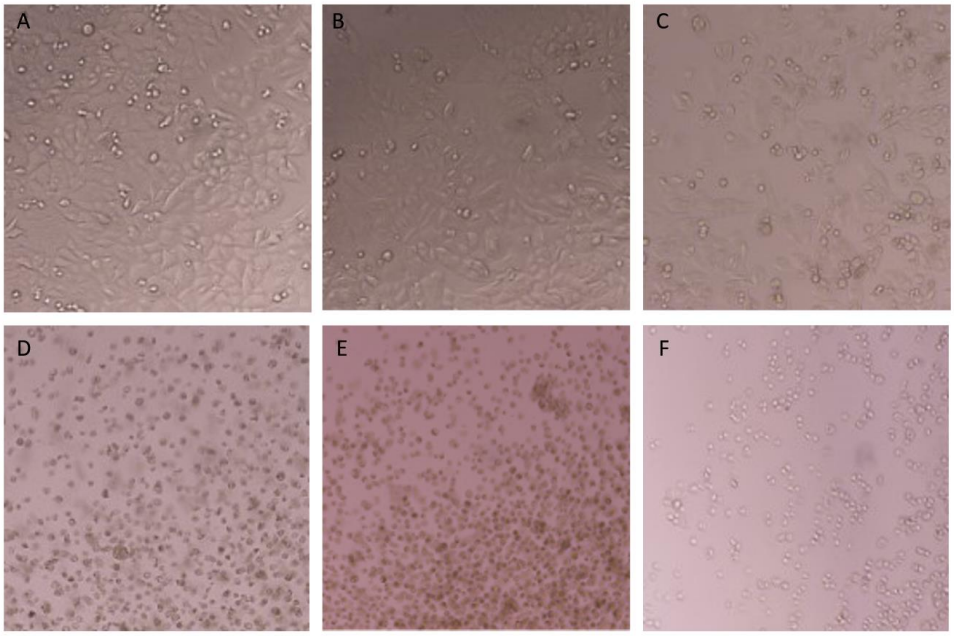

Figure 4. 8. T98G cells on TCPS after 48h culture (10X) a) Control b) 1 µM c) 2 µM d) 4 µM e) 6 µM f) 8 µM.

4.2. Production of Chitosan Hydrogels

Hydrogels were produced in a 24-well cell culture dish with 200 µL of hydrogel per well. In order to ensure the pH and salt balance in which the cells can live before the hydrogels are taken into cell culture, 500 µL of different cell media (DMEM-F12 and DMEM-High glucose) is placed for each well after gelation. It was decided that the most suitable cell culture medium was DMEM-F12 without Hepes. In the experiments, it was determined that the hydrogels conditioned in the incubator by adding cell medium after gelation reacted with the cell medium and the color of the cell medium changed from pink to green. Figure 4.7 below shows the conditioning of genipin and glycerol phosphate at different concentrations before and after gelation, as well as conditioning of these tested concentrations in different culture media.

Table 4.1.Parameters for hydrogel optimization

Concentration of Genipin (mM)	**Glycerol phosphate (µL)**	**Acidic acid (%)**
1 mM	100	0.5
1 mM	200	1
1 mM	250	1
1 mM	300	1
1.25 mM	200	1
1.5 mM	200	1
1.5 mM	300	1
2 mM	200	1
	Selected Hydrogel Condition	
1 mM	**100**	**0.5**

Color difference was observed in hydrogels produced under different conditions. It was observed that in the lighter color condition, in direct proportion to the color difference, fragmentation was more common in the cell medium (Figure 4.10). As a result of the optimization of hydrogel production, the condition without any dispersion in the cell medium or which does not change the acidity of the cell medium was chosen. Consequently, 0.5% acidic acid, 100 µL Glycerol phosphate and 1 mM Genipin were preferred for each 5 mL hydrogel production among the produced hydrogels at different concentrations, and analyzes were made on this hydrogel.

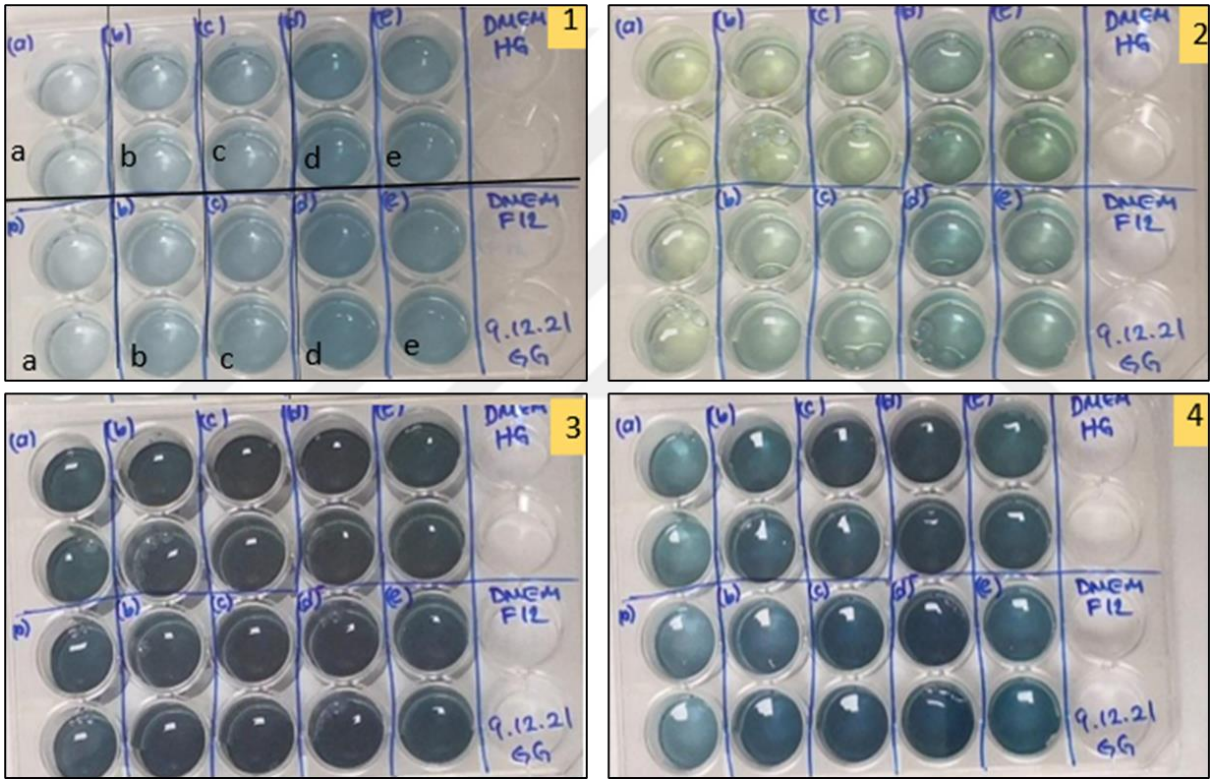

Figure 4.9. Production and color changes of the hydrogels 1) After 2 hours of gelation 2) After the culture medium added after gelation 3) The color of the culture medium after 1 day of conditioning 4) After the removal of the culture medium after 1 day

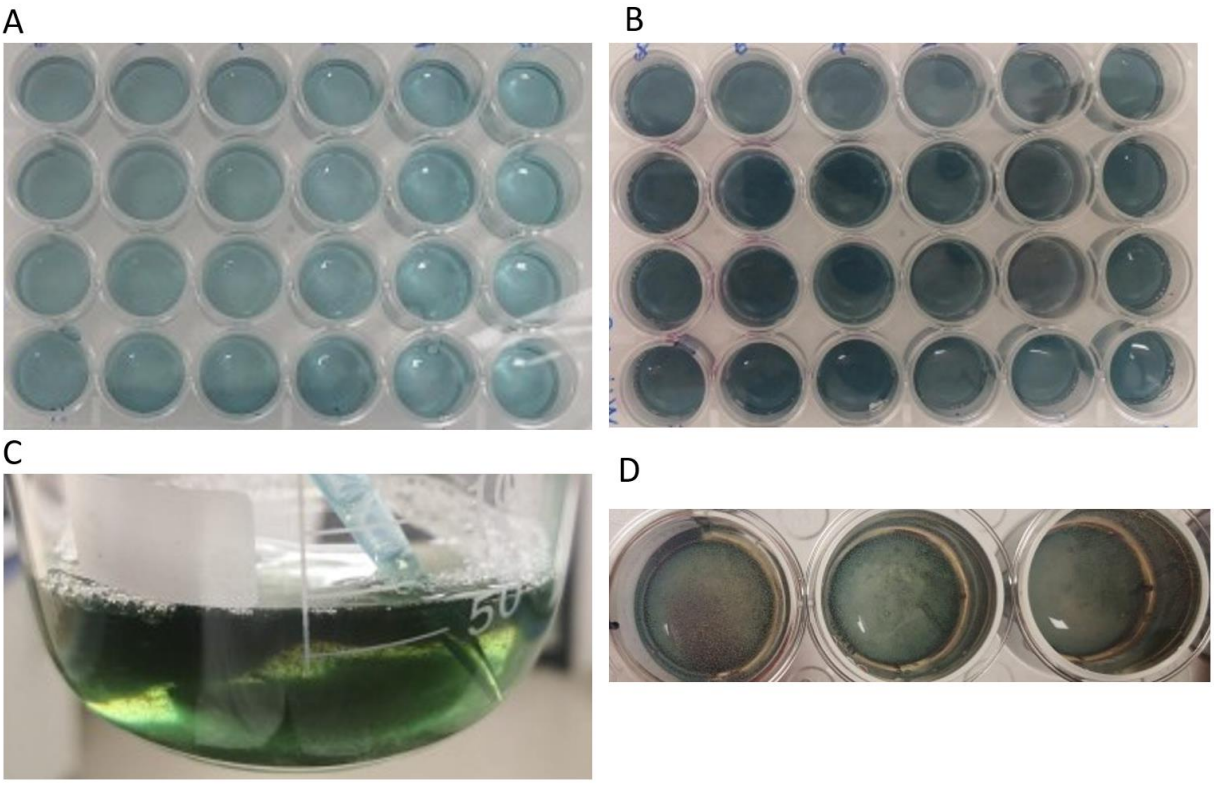

Figure 4.10.Gel Production A) After 2.30 hours of gelling B) After conditioning in cell culture medium for 1 day C) Color of the cell culture medium collected on the gel after conditioning D) Close-up view of the fragmented gels (1 mM genipin, 0.5% containing 200 µL glycerol phosphate 2% w/v chitosan dissolved in acetic acid).

4.2.1. Morphology Analysis

Networks of interconnected porous scaffolds are necessary for cell proliferation and migration, waste clearance, and nutrition transfer. The ultimate mechanical properties of the scaffold are determined by the porosity and pore size, which also affect cell activity [64].

The morphology of hydrogel was analyzed by scanning electron microscopy (SEM). The hydrogels were frozen at -80ºC after gelation, and in two different materials, 24 well plate and syringe. Figure 4.9 and 4.10 show the porous structure of the hydrogel containing 0.5% acidic acid, 100 µL glycerol phosphate and 1 mM genipin used in the experiments. Both hydrogels showed porous structure. The material that they were prepared in affected the pore structure of the hydrogels. The pore diameter distributions were calculated by Image J program and given in Figure 4.11. Average pore diameter was calculated as 422 ± 140 nm for the hydrogels

produced in 24 well plate and 341 ± 91nm for the hydrogels produced in syringe. The hydrogels prepared in the syringe showed more smaller pore diameters when compared to the hydrogels produced in 24 well plate.

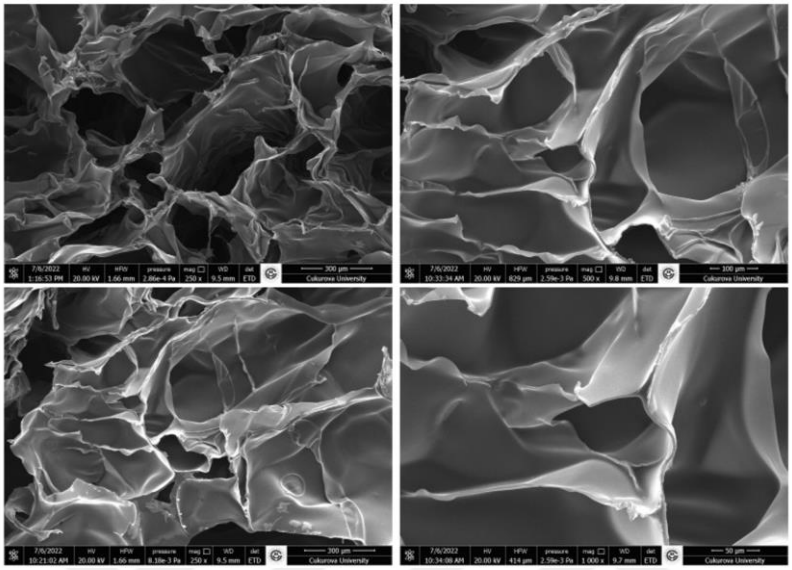

Figure 4.11. SEM images of freeze-dried 2.5D chitosan hydrogels in 24 well plate (250X, 500X, 1000X).

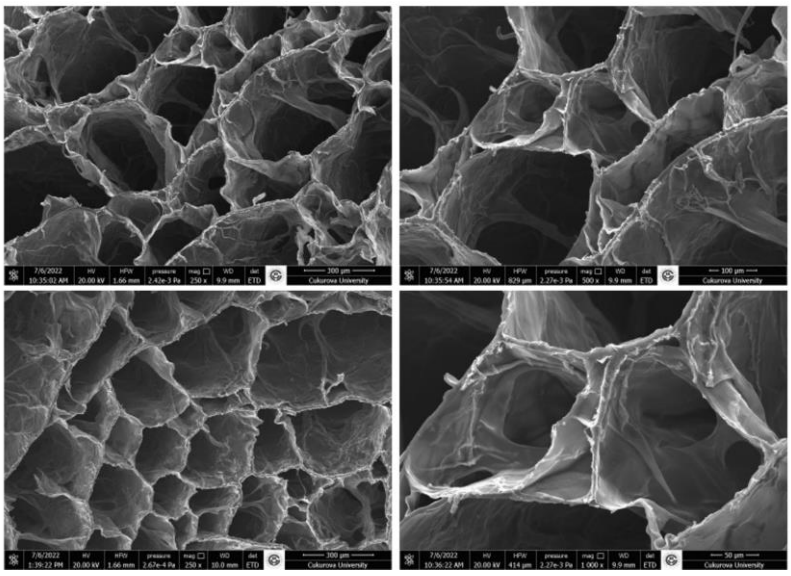

Figure 4.12. SEM images of freeze-dried 2.5D chitosan hydrogels in syringe (250X, 500X, 1000X).

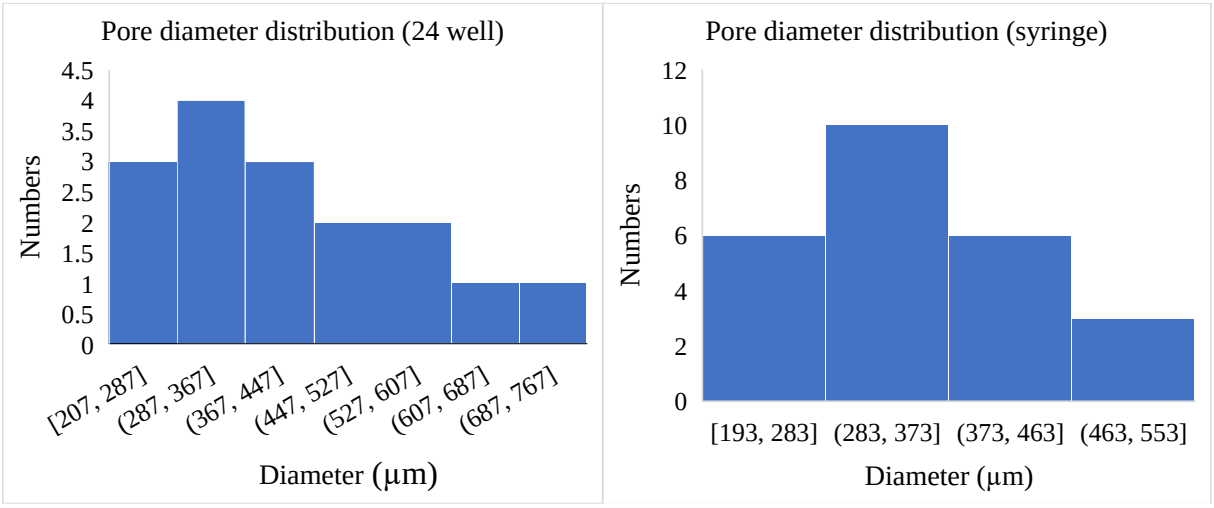

Figure 4. 13. Pore diameter distribution of 2.5D chitosan hydrogels.

4.3. Culture of T98G Cells on 2.5D Chitosan Hydrogels

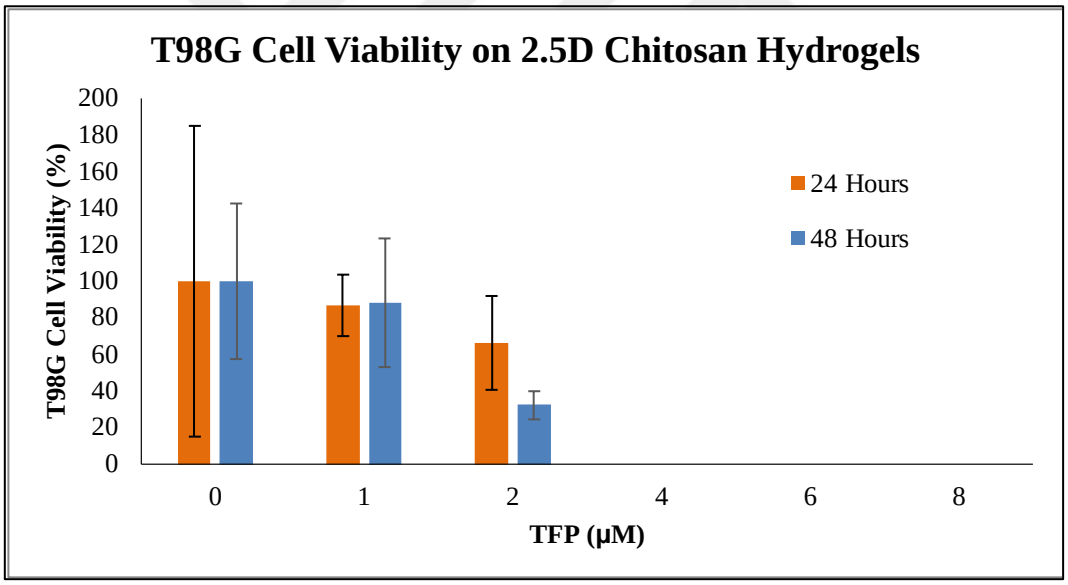

Figure 4. 14. Effect of TFP on T98G cell proliferation in a dose- and time-dependent manner on hydrogels.

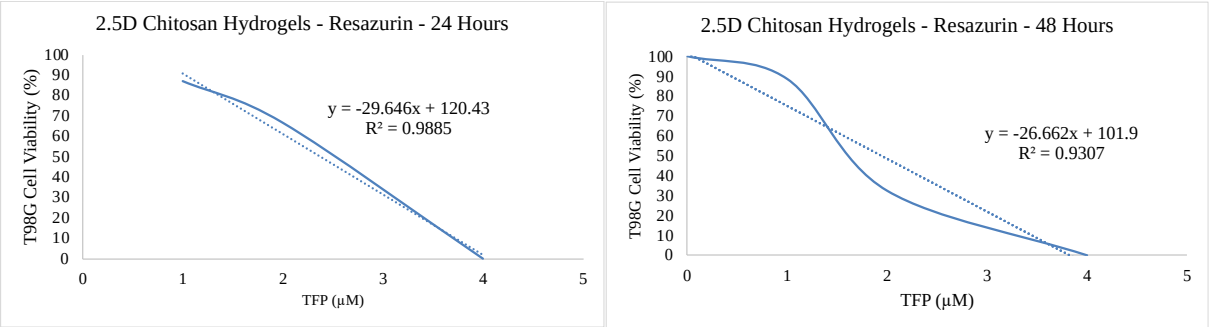

Figure 4. 15. Resazurin analysis results on 2.5D chitosan hydrogels at 24 h and 48 h.

2D studies have led to pioneering results in the complex relationship between cell structure and cellular microenvironment interactions [4]. It is important to simulate *in vivo* like environment for natural normal or tumor tissue structures for decreasing workload in preclinical and clinical studies [7]. The 24-hour and 48-hour cell viability of TFP concentration on 2.5D chitosan hydrogels is given in Figure 4.12. T98G cells on the hydrogel were found to be more sensitive to TFP concentration than cells in the TCPS group. There was no cell viability at 4 µM TFP dose both for 24 and 48 h. The viability of the 2 µM concentration in the TCPS group, which was about 80%, decreased to 60% on the hydrogel. Dose that causes 50% cell death compared to control IC50 value expressed as 2.37 µM in 24 hours; IC50 of 48 hours was determined as 1.94 µM (Figure 4.13).

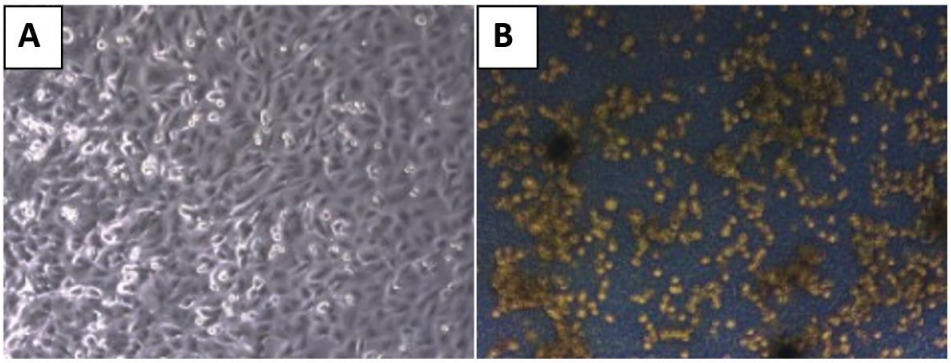

Figure 4. 16. Morphology of T98G cells on TCPS, 10x (A) and on 2.5D chitosan hydrogels 10x (B).

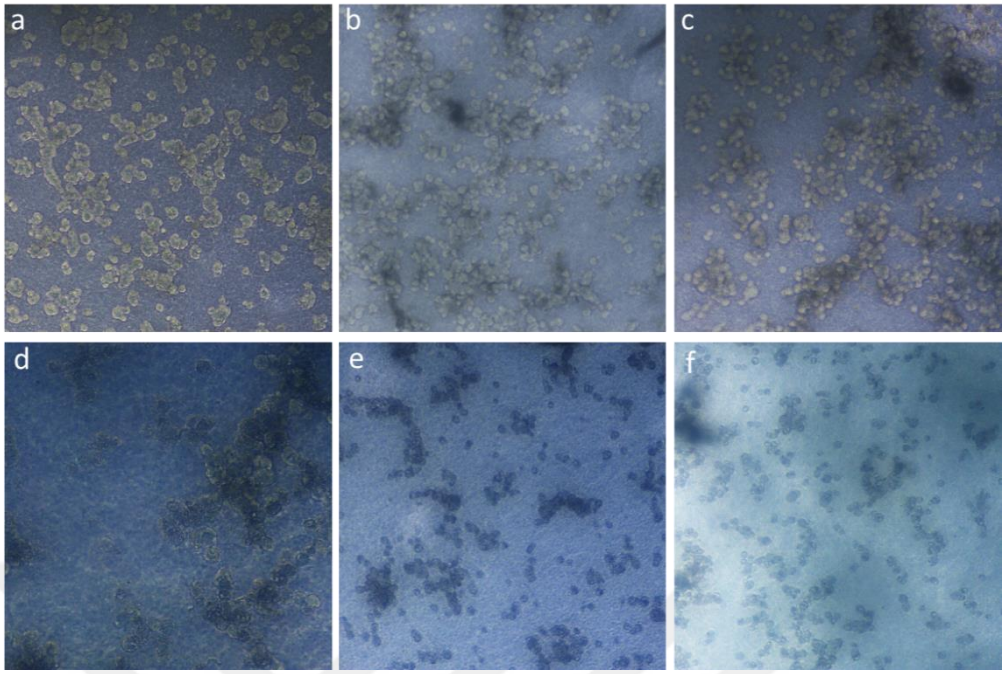

Figure 4. 17. T98G cells on 2.5D chitosan hydrogels after 24 h culture (10X) a) Hydrogel control b) 1 µM c) 2 µM d) 4 µM e) 6 µM f) 8 µM.

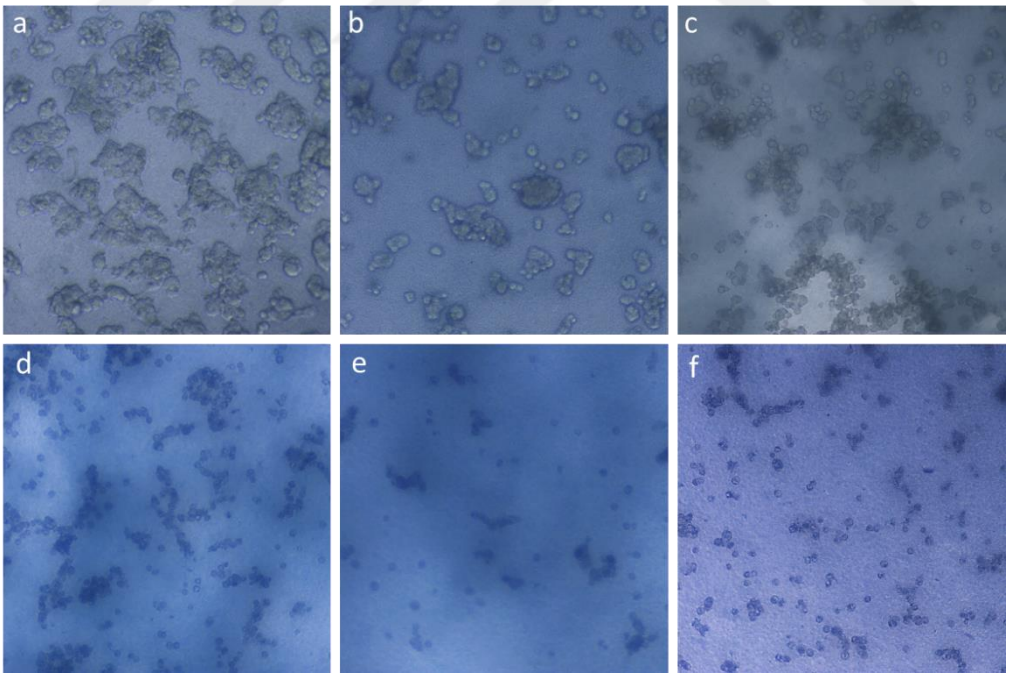

Figure 4. 18. T98G cells on 2.5D chitosan hydrogels after 48-hour culture (10X) a) Hydrogel control b) 1 µM c) 2 µM d) 4 µM e) 6 µM f) 8 µM.

Table 4. 2. IC50 values of TFP on T98G cell line

	2D on TCPS		2.5D on Chitosan Hydrogels	TFP Drug Concentration
	MTT	**Resazurin**	**Resazurin**	
24h	3.75	2.86	2.37	0-20 μM (0,1,2,4,6,8,10,20)
48h	2.57	2.64	1.94	

Manome et al., studied the characterization of glioblastoma cells in 3D culture including T98G cells. They showed that in the 3D culture environment of the T98G cell line, its fibers fill the extracellular spaces. They also proved that cells tend to migrate and proliferate into empty spaces. In 3D environments, cells migrated to neighboring areas where they produced more extracellular matrix and simultaneously the cells had fully attached to the scaffold [65].

Abugomaa et al. established a 2.5D culture model using cancer cells from dogs and cats in the presence of Matrigel. Cells cultured in 2.5D medium showed better adhesion, growth, and faster proliferation rate compared to cells cultured in normal TCPS medium. Compared to normal 2D cell line media, 2.5D media showed stable transitions and a higher proliferation rate. [47].

Kojima et al. also used Matrigel to create a 2.5D culture medium in their study. The culture medium created was 2.5D culture, which is similar to human organoids *in vivo* and more sensitive to changes induced by various stimuli than that of 2D culture. Thus, it may be a useful *in vitro* model for studying the mechanisms of human disease [66].

The Table 4.3. shows the IC50 values of TFP on different cell lines after 24 h and 48 h culture on TCPS. In this study, IC50 values of TFP on T98G cell line were lower both on 2D and 2.5D cell cultures at 24 h and 48 h when compared to the literature values given in Table 4.3.

In this thesis, T98G cells on 2.5D chitosan hydrogels were shown to be slightly sensitive compared to the 2D cell culture on TCPS. MTT analysis and resazurin results showed that chitosan hydrogels formed a 2.5D environment more proliferative than TCPS due to its highly porous surface. In future studies, different cell lines and related drugs can be studied in this 2.5D chitosan hydrogel culture system.

Table 4. 3. IC50 values of TFP on different cell lines

Cell Line	TFP Concentration (μM)	Hours of Treatment (h)	IC50 Values (μM)	References
U251	0-30 μM (± 2.5)	24h	16	[67]
U87			15	
P3			15.5	
MiaPaCa-2	0-30 μM (±5)	24h	13.24	[19]
1008			10.46	
HN01			14.78	
JIPC			11.45	
LIPC			15.07	
CT26	0-20 μM (0,2.5,5,10,20)	48h	16.8	[68]
HCT116			16.2	
SW620			13.9	
A549	0-20 μM (1,2,5,10,20)	48h	14.36	[69]
T98G	0-20 μM (1,2,5,10,20)	48h	10-20	[70]

4.4. Immunofluorescent Staining ((4', 6-diamidino-2-phenylindole) DAPI Staining)

The nuclei of the cells were counterstained with DAPI on TCPS (Figure 4.19). The cell concentration in 2 μM TFP applied group was higher when compared to 4 μM TFP applied group, however, there were some changes in the shape of the nuclei. Nuclei of T98G cells in control group without TFP showed elliptical like shape. After TFP application, there were some condensations and crescent like nuclei.

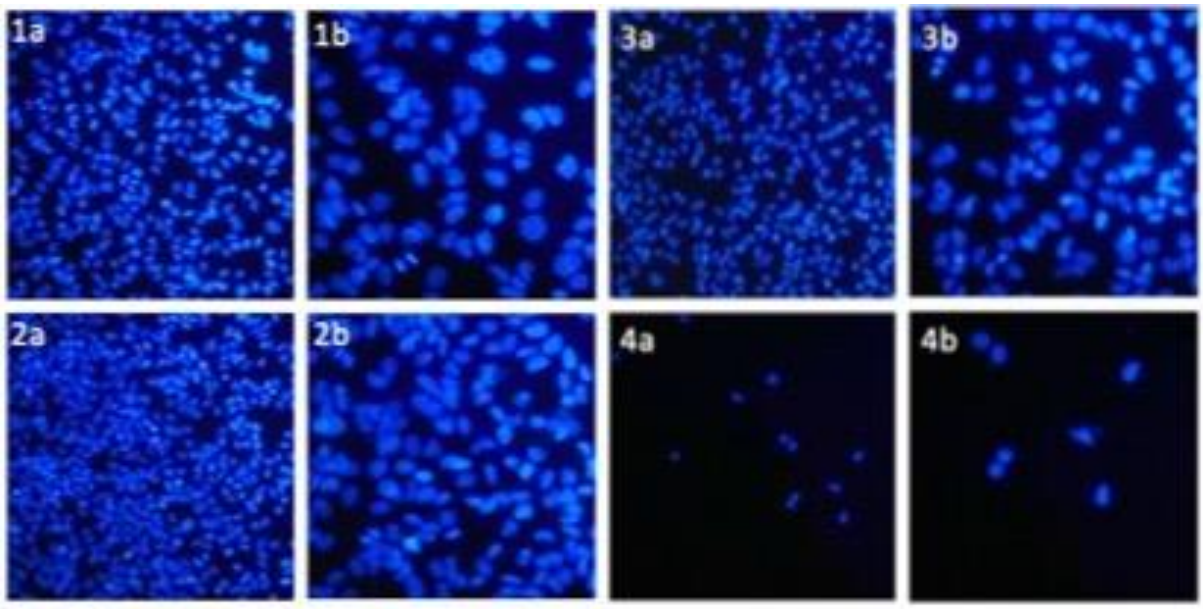

Figure 4. 19. DAPI staining images of T98G cells cultured on TCPS for 24 h: 1- Control, 2- 1 µM TFP, 3- 2 µM TFP, 4- 4 µM TFP; (a)10X, (b) 20X.

As seen in Figure 4.20, In the image taken from the hydrogel control group, the nuclei of the cells cannot be clearly distinguished. It was more visible towards the interior of the hydrogel in visual analysis under fluorescence microscopy. Thin sections should be taken from the produced hydrogel and it should be checked whether the cell migrates or not. In the study, it is thought that the cells migrate towards the inner parts and, accordingly, are more sensitive to the drug response.

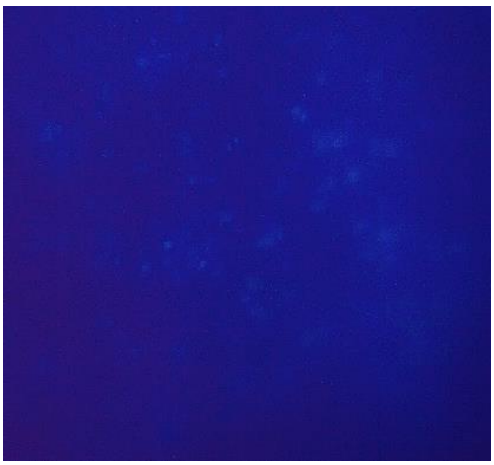

Figure 4. 20. DAPI staining images of T98G cells cultured on Hydrogel

5. CONCLUSION

In this thesis, we aimed to compare the effect of 2D and 2.5D microenvironment on Trifluoperazine (TFP) drug dose response of T98G cell line. T98G cells are a human glioblastoma cell line used as experimental models to improve cancer treatment modalities. TFP is an FDA-approved antipsychotic and antiemetic drug used to treat schizophrenia. There is limited study showing the effects of TFP on T98G cell line. Here, a 2.5D cell culture system was developed using chitosan-glycerol phosphate-genipin hydrogels to investigate the effects of TFP on the T98G cell line compared to the 2D cell culture system on TCPS.

The IC50 concentrations of TFP on T98G cell line was calculated as 3.75 μM for 24 h and 2.57 μM for 48 h by MTT analysis for 2D culture on TCPS. IC50 concentrations of TFP on T98G cell line was calculated as 2.86 μM for 24 h and 2.64 μM for 48 h by resazurin analysis for 2D culture on TCPS. It was concluded that, IC50 concentrations calculated from MTT and resazurin analysis results were very close. DAPI staining also showed the condensed and small nuclei shape in T98G cells after 24 h application of TFP when compared to the control group. According to these results TFP doses were selected as 1-8 μM for 2.5D cell culture studies.

2.5D chitosan hydrogels were prepared at selected conditions to obtain stable wet hydrogels in the cell culture studies. 0.5% acidic acid as a solvent, 100 μL glycerol phosphate (1 g/mL) and 1 mM genipin as physical and chemical crosslinkers were preferred for hydrogel production. T98G cells were cultured on these hydrogels for 24 and 48 h. Viability of the cells were both determined by resazurin analysis. IC50 concentration of TFP for T98G cells cultured on 2.5D chitosan hydrogels were determined as 2.37 μM for 24 h culture and 1.94 μM for 48 h culture.

In conclusion, developed 2.5D chitosan hydrogels exhibit 3D like properties. IC50 calculations indicated that T98G cells were slightly sensitive to TFP on 2.5D chitosan hydrogels when compared to 2D culture on TCPS. In future studies, different cell lines can be studied on these 2.5D chitosan hydrogels with different drug molecules to show the potential of these hydrogels to be used in drug response studies as 3D like microenvironment.

REFERENCES

[1] C. Jensen and Y. Teng, ‘Is It Time to Start Transitioning From 2D to 3D Cell Culture?’, *Front Mol Biosci*, vol. 7, p. 33, Mar. 2020, doi: 10.3389/fmolb.2020.00033.

[2] K. Duval *et al.*, ‘Modeling Physiological Events in 2D vs. 3D Cell Culture’, 2017, doi: 10.1152/physiol.00036.2016.

[3] M. W. Tibbitt and K. S. Anseth, ‘Hydrogels as extracellular matrix mimics for 3D cell culture’, *Biotechnology and Bioengineering*, vol. 103, no. 4. pp. 655–663, Jul. 01, 2009. doi: 10.1002/bit.22361.

[4] N. Jaiswal, S. E. Haynesworth, A. I. Caplan, and S. P. Bruder, ‘Osteogenic differentiation of purified, culture-expanded human mesenchymal stem cells in vitro’, *J Cell Biochem*, vol. 64, no. 2, pp. 295–312, Feb. 1997, doi: 10.1002/(SICI)1097-4644(199702)64:2<295::AID-JCB12>3.0.CO;2-I.

[5] M. W. Hess, K. Pfaller, H. L. Ebner, B. Beer, D. Hekl, and T. Seppi, *3D versus 2D cell culture. Implications for electron microscopy*, vol. 96, no. C. Academic Press, 2010. doi: 10.1016/S0091-679X(10)96027-5.

[6] M. Kapałczyńska *et al.*, ‘2D and 3D cell cultures – a comparison of different types of cancer cell cultures’, *undefined*, vol. 14, no. 4, pp. 910–919, 2018, doi: 10.5114/AOMS.2016.63743.

[7] N. Gupta, J. R. Liu, B. Patel, D. E. Solomon, B. Vaidya, and V. Gupta, ‘Microfluidics-based 3D cell culture models: Utility in novel drug discovery and delivery research’, *Bioeng Transl Med*, vol. 1, no. 1, pp. 63–81, Mar. 2016, doi: 10.1002/btm2.10013.

[8] E. C. Holland, ‘Glioblastoma multiforme: The terminator’, *Proceedings of the National Academy of Sciences of the United States of America*, vol. 97, no. 12. pp. 6242–6244, Jun. 06, 2000. doi: 10.1073/pnas.97.12.6242.

[9] M. E. Oraiopoulou *et al.*, ‘A 3D tumor spheroid model for the T98G Glioblastoma cell line phenotypic characterization’, *Tissue Cell*, vol. 59, pp. 39–43, Aug. 2019, doi: 10.1016/j.tice.2019.05.007.

[10] A. Roniotis, K. Marias, V. Sakkalis, and M. Zervakis, ‘Diffusive modelling of glioma evolution: a review’, *J Biomed Sci Eng*, vol. 03, no. 05, pp. 501–508, 2010, doi: 10.4236/jbise.2010.35070.

[11] Y. Xie *et al.*, ‘The Human Glioblastoma Cell Culture Resource: Validated Cell Models Representing All Molecular Subtypes’, *EBioMedicine*, vol. 2, no. 10, pp. 1351–1363, Oct. 2015, doi: 10.1016/j.ebiom.2015.08.026.

[12] G. H. Stein, ‘T98G: An anchorage-independent human tumor cell line that exhibits stationary phase G1 arrest in vitro’, *J Cell Physiol*, vol. 99, no. 1, pp. 43–54, 1979, doi: 10.1002/jcp.1040990107.

[13] V. Adamski, A. D. Schmitt, C. Flüh, M. Synowitz, K. Hattermann, and J. Held-Feindt, ‘Isolation and characterization of fast-migrating human glioma cells in the progression of malignant gliomas’, *Oncol Res*, vol. 25, no. 3, pp. 341–353, 2017, doi: 10.3727/096504016X14737243054982.

[14] L. N. Kiseleva, A. V. Kartashev, N. L. Vartanyan, A. A. Pinevich, and M. P. Samoilovich, ‘A172 and T98G cell lines characteristics’, *Cell tissue biol*, vol. 10, no. 5, pp. 341–348, Sep. 2016, doi: 10.1134/S1990519X16050072.

[15] Chen, ‘Molecular mechanism of trifluoperazine induces apoptosis in human A549 lung adenocarcinoma cell lines’, *Mol Med Rep*, vol. 2, no. 5, pp. 811–817, Jul. 2009, doi: 10.3892/mmr_00000177.

[16] S. Kang *et al.*, ‘Cancer Biology and Signal Transduction Trifluoperazine, a Well-Known Antipsychotic, Inhibits Glioblastoma Invasion by Binding to Calmodulin and Disinhibiting Calcium Release Channel IP 3 R’, *Mol Cancer Ther*, vol. 16, no. 1, 2017, doi: 10.1158/1535-7163.MCT-16-0169-T.

[17] Ü. Abdülrezzak, Z. Erdogan, G. Silov, A. Özdal, and Ö. Turhal, ‘Effect of trifluoperazine on Tc-99m sestamibi uptake in patients with advanced nonsmall cell lung cancer’, *Indian Journal of Nuclear Medicine*, vol. 31, no. 2, pp. 103–107, Apr. 2016, doi: 10.4103/0972-3919.178256.

[18] Z. Feng *et al.*, ‘The antipsychotic agent trifluoperazine hydrochloride suppresses triple-negative breast cancer tumor growth and brain metastasis by inducing G0/G1 arrest and apoptosis’, *Cell Death Dis*, vol. 9, no. 10, Oct. 2018, doi: 10.1038/s41419-018-1046-3.

[19] C. Huang, W. Lan, N. Fraunhoffer, A. Meilerman, J. Iovanna, and P. Santofimia-Castaño, ‘Dissecting the anticancer mechanism of trifluoperazine on pancreatic ductal adenocarcinoma’, *Cancers (Basel)*, vol. 11, no. 12, Dec. 2019, doi: 10.3390/cancers11121869.

[20] K. Qian *et al.*, ‘Trifluoperazine as an alternative strategy for the inhibition of tumor growth of colorectal cancer’, *J Cell Biochem*, vol. 120, no. 9, pp. 15756–15765, Sep. 2019, doi: 10.1002/jcb.28845.

[21] S. Kang *et al.*, ‘Repositioning of the antipsychotic trifluoperazine: Synthesis, biological evaluation and in silico study of trifluoperazine analogs as anti-glioblastoma agents’, *Eur J Med Chem*, vol. 151, pp. 186–198, May 2018, doi: 10.1016/j.ejmech.2018.03.055.

[22] M. E. Smithmyer, S. E. Cassel, and A. M. Kloxin, ‘Bridging 2D and 3D culture: Probing impact of extracellular environment on fibroblast activation in layered hydrogels’, *AIChE Journal*, vol. 65, no. 12, Dec. 2019, doi: 10.1002/aic.16837.

[23] C. A. Pickover, ‘Surfing through hyperspace : understanding higher universes in six easy lessons’, p. 239, 1999.

[24] M. J. Bissell and D. Bilder, ‘Polarity determination in breast tissue: desmosomal adhesion, myoepithelial cells, and laminin 1’, *Breast Cancer Research*, vol. 5, no. 2, p. 117, 2003, doi: 10.1186/BCR579.

[25] E. Assémat, E. Bazellières, E. Pallesi-Pocachard, A. Le Bivic, and D. Massey-Harroche, ‘Polarity complex proteins’, *Biochimica et Biophysica Acta (BBA) - Biomembranes*, vol. 1778, no. 3, pp. 614–630, Mar. 2008, doi: 10.1016/J.BBAMEM.2007.08.029.

[26] J. Chen and M. Zhang, ‘The Par3/Par6/aPKC complex and epithelial cell polarity’, *Exp Cell Res*, vol. 319, no. 10, pp. 1357–1364, Jun. 2013, doi: 10.1016/J.YEXCR.2013.03.021.

[27] A. C. Ribeiro-filho, D. Levy, J. L. M. Ruiz, M. da C. Mantovani, and S. P. Bydlowski, ‘Traditional and Advanced Cell Cultures in Hematopoietic Stem Cell Studies’, *Cells 2019, Vol. 8, Page 1628*, vol. 8, no. 12, p. 1628, Dec. 2019, doi: 10.3390/CELLS8121628.

[28] P. Friedl, J. Locker, E. Sahai, and J. E. Segall, ‘Classifying collective cancer cell invasion’, *Nature Cell Biology*, vol. 14, no. 8. pp. 777–783, Aug. 2012. doi: 10.1038/ncb2548.

[29] K. L. Schmeichel and M. J. Bissell, ‘Modeling tissue-specific signaling and organ function in three dimensions’, *J Cell Sci*, vol. 116, no. Pt 12, pp. 2377–2388, Jun. 2003, doi: 10.1242/JCS.00503.

[30] Q. L. Loh and C. Choong, ‘Three-Dimensional Scaffolds for Tissue Engineering Applications: Role of Porosity and Pore Size’, *Tissue Eng Part B Rev*, 2013, doi: 10.1089/ten.teb.2012.0437.

[31] M. Ravi, V. Paramesh, S. R. Kaviya, E. Anuradha, and F. D. Paul Solomon, ‘3D cell culture systems: Advantages and applications’, *J Cell Physiol*, vol. 230, no. 1, pp. 16–26, Jan. 2015, doi: 10.1002/jcp.24683.

[32] R. Edmondson, J. J. Broglie, A. F. Adcock, and L. Yang, ‘Three-dimensional cell culture systems and their applications in drug discovery and cell-based biosensors’, *Assay and Drug Development Technologies*, vol. 12, no. 4. Mary Ann Liebert Inc., pp. 207–218, May 01, 2014. doi: 10.1089/adt.2014.573.

[33] H. Baharvand, S. M. Hashemi, S. K. Ashtiani, and A. Farrokhi, ‘Differentiation of human embryonic stem cells into hepatocytes in 2D and 3D culture systems in vitro’, *International Journal of Developmental Biology*, vol. 50, no. 7, pp. 645–652, 2006, doi: 10.1387/ijdb.052072hb.

[34] P. D. Benya and J. D. Shaffer, ‘Dedifferentiated chondrocytes reexpress the differentiated collagen phenotype when cultured in agarose gels’, *Cell*, vol. 30, no. 1, pp. 215–224, 1982, doi: 10.1016/0092-8674(82)90027-7.

[35] C. M. Nelson and M. J. Bissell, ‘Modeling dynamic reciprocity: Engineering three-dimensional culture models of breast architecture, function, and neoplastic transformation’, *Seminars in Cancer Biology*, vol. 15, no. 5 SPEC. ISS. Academic Press, pp. 342–352, 2005. doi: 10.1016/j.semcancer.2005.05.001.

[36] D. Lv, Z. Hu, L. Lu, H. Lu, and X. Xu, ‘Three-dimensional cell culture: A powerful tool in tumor research and drug discovery’, *Oncology Letters*, vol. 14, no. 6. Spandidos Publications, pp. 6999–7010, Dec. 01, 2017. doi: 10.3892/ol.2017.7134.

[37] C. S. Szot, C. F. Buchanan, J. W. Freeman, and M. N. Rylander, ‘3D in vitro bioengineered tumors based on collagen I hydrogels’, *Biomaterials*, vol. 32, no. 31, pp. 7905–7912, Nov. 2011, doi: 10.1016/J.BIOMATERIALS.2011.07.001.

[38] J. E. Barralet, L. Wang, M. Lawson, J. T. Triffitt, P. R. Cooper, and R. M. Shelton, ‘Comparison of bone marrow cell growth on 2D and 3D alginate hydrogels’, *Journal of Materials Science: Materials in Medicine 2005 16:6*, vol. 16, no. 6, pp. 515–519, Jun. 2005, doi: 10.1007/S10856-005-0526-Z.

[39] C. R. Thoma, M. Zimmermann, I. Agarkova, J. M. Kelm, and W. Krek, ‘3D cell culture systems modeling tumor growth determinants in cancer target discovery’, *Adv Drug Deliv Rev*, vol. 69–70, pp. 29–41, Apr. 2014, doi: 10.1016/J.ADDR.2014.03.001.

[40] C. Hsiao, M. Tomai, J. Glynn, and S. P. Palecek, ‘Effects of 3D microwell culture on initial fate specification in human embryonic stem cells’, *AIChE J*, vol. 60, no. 4, p. 1225, Apr. 2014, doi: 10.1002/AIC.14351.

[41] K. Ziółkowska, A. Stelmachowska, R. Kwapiszewski, M. Chudy, A. Dybko, and Z. Brzózka, ‘Long-term three-dimensional cell culture and anticancer drug activity evaluation in a microfluidic chip’, *Biosens Bioelectron*, vol. 40, no. 1, pp. 68–74, Feb. 2013, doi: 10.1016/J.BIOS.2012.06.017.

[42] X. Xu, M. C. Farach-Carson, and X. Jia, ‘Three-dimensional in vitro tumor models for cancer research and drug evaluation’, *Biotechnol Adv*, vol. 32, no. 7, pp. 1256–1268, Nov. 2014, doi: 10.1016/J.BIOTECHADV.2014.07.009.

[43] M. P. Pebworth, S. A. Cismas, and P. Asuri, ‘A novel 2.5D culture platform to investigate the role of stiffness gradients on adhesion-independent cell migration’, *PLoS One*, vol. 9, no. 10, Oct. 2014, doi: 10.1371/journal.pone.0110453.

[44] J. E. Marszalek, C. G. Simon, C. Thodeti, R. K. Adapala, A. Murthy, and A. Karim, ‘2.5D constructs for characterizing phase separated polymer blend surface morphology in tissue engineering scaffolds’, *J Biomed Mater Res A*, vol. 101 A, no. 5, pp. 1502–1510, 2013, doi: 10.1002/jbm.a.34439.

[45] J. L. Curley, S. R. Jennings, and M. J. Moore, ‘Fabrication of micropatterned hydrogels for neural culture systems using dynamic mask projection photolithography.’, *J Vis Exp*, no. 48, p. 2636, Feb. 2011, doi: 10.3791/2636.

[46] H. Lam, ‘3D co-culture spheroid drug screening platform for pancreatic cancer invasion’, 2017.

[47] A. Abugomaa *et al.*, ‘Establishment of 2.5D organoid culture model using 3D bladder cancer organoid culture’, *Sci Rep*, vol. 10, no. 1, pp. 1–13, Dec. 2020, doi: 10.1038/s41598-020-66229-w.

[48] A. De La Zerda, M. J. Kratochvil, N. A. Suhar, and S. C. Heilshorn, ‘Review: Bioengineering strategies to probe T cell mechanobiology’, *APL Bioeng*, vol. 2, no. 2, pp. 1–27, 2018, doi: 10.1063/1.5006599.

[49] M. Jhanwar-Uniyal, M. Labagnara, M. Friedman, A. Kwasnicki, and R. Murali, ‘Glioblastoma: Molecular Pathways, Stem Cells and Therapeutic Targets’, *Cancers (Basel)*, vol. 7, no. 2, p. 538, 2015, doi: 10.3390/CANCERS7020538.

[50] O. Van Tellingen, B. Yetkin-Arik, M. C. De Gooijer, P. Wesseling, T. Wurdinger, and H. E. De Vries, ‘Overcoming the blood-brain tumor barrier for effective glioblastoma treatment’, *Drug Resist Updat*, vol. 19, pp. 1–12, Mar. 2015, doi: 10.1016/J.DRUP.2015.02.002.

[51] Y. Xie *et al.*, ‘The Human Glioblastoma Cell Culture Resource: Validated Cell Models Representing All Molecular Subtypes’, *EBioMedicine*, vol. 2, no. 10, pp. 1351–1363, Oct. 2015, doi: 10.1016/j.ebiom.2015.08.026.

[52] S. Pedron, E. Becka, and B. A. C. Harley, ‘Regulation of glioma cell phenotype in 3D matrices by hyaluronic acid’, *Biomaterials*, vol. 34, no. 30, pp. 7408–7417, Oct. 2013, doi: 10.1016/J.BIOMATERIALS.2013.06.024.

[53] M. Wiranowska, M. V. Rojiani, M. Wiranowska, and M. V. Rojiani, ‘Extracellular Matrix Microenvironment in Glioma Progression’, *Glioma - Exploring Its Biology and Practical Relevance*, Nov. 2011, doi: 10.5772/24666.

[54] S. C. Gupta, B. Sung, S. Prasad, L. J. Webb, and B. B. Aggarwal, ‘Cancer drug discovery by repurposing: teaching new tricks to old dogs’, *Trends Pharmacol Sci*, vol. 34, no. 9, pp. 508–517, Sep. 2013, doi: 10.1016/J.TIPS.2013.06.005.

[55] D. M. Gardner, R. J. Baldessarini, and P. Waraich, ‘Modern antipsychotic drugs: a critical overview’, *CMAJ*, vol. 172, no. 13, pp. 1703–1711, Jun. 2005, doi: 10.1503/CMAJ.1041064.

[56] H. Buschmann, J. L. Díaz, J. Holenz, A. Párraga, A. Torrens, and J. M. Vela, *Antidepressants, Antipsychotics, Anxiolytics: From Chemistry and Pharmacology to Clinical Application*, vol. 1–2. Wiley-VCH, 2008. doi: 10.1002/9783527619337.

[57] M. Dold, M. T. Samara, C. Li, M. Tardy, and S. Leucht, ‘Haloperidol versus first-generation antipsychotics for the treatment of schizophrenia and other psychotic disorders’, *Cochrane Database Syst Rev*, vol. 1, no. 6, Jan. 2015, doi: 10.1002/14651858.CD009831.PUB2.

[58] A. Jaszczyszyn *et al.*, ‘Chemical structure of phenothiazines and their biological activity’, *Pharmacol Rep*, vol. 64, no. 1, pp. 16–23, 2012, doi: 10.1016/S1734-1140(12)70726-0.

[59] L. Qi and Y. Q. Ding, ‘Potential antitumor mechanisms of phenothiazine drugs’, *Sci China Life Sci*, vol. 56, no. 11, pp. 1020–1027, Nov. 2013, doi: 10.1007/S11427-013-4561-6.

[60] H. J. Jung, J. H. Kim, J. S. Shim, and H. J. Kwon, ‘A Novel Ca2+/Calmodulin Antagonist HBC Inhibits Angiogenesis and Down-regulates Hypoxia-inducible Factor’, *J Biol Chem*, vol. 285, no. 33, p. 25867, Aug. 2010, doi: 10.1074/JBC.M110.135632.

[61] R. Carneiro Borra Mônica Andrade Lotufo Sonia Maria Gagioti Fabiana de Mesquita Barros Priscila Maria Andrade, G. Student -Graduate Program in Biodentistry, and R. Carneiro Borra, ‘A simple method to measure cell viability in proliferation and cytotoxicity assays Histology’, 2009.

[62] S. Kang *et al.*, ‘Trifluoperazine, a Well-Known Antipsychotic, Inhibits Glioblastoma Invasion by Binding to Calmodulin and Disinhibiting Calcium Release Channel IP3R’, *Mol Cancer Ther*, vol. 16, no. 1, pp. 217–227, Jan. 2017, doi: 10.1158/1535-7163.MCT-16-0169-T.

[63] X. Zhang *et al.*, ‘Trifluoperazine, a novel autophagy inhibitor, increases radiosensitivity in glioblastoma by impairing homologous recombination’, *Journal of Experimental and Clinical Cancer Research*, vol. 36, no. 1, Sep. 2017, doi: 10.1186/s13046-017-0588-z.

[64] Q. L. Loh and C. Choong, ‘Three-dimensional scaffolds for tissue engineering applications: Role of porosity and pore size’, *Tissue Engineering - Part B: Reviews*, vol. 19, no. 6. pp. 485–502, Dec. 01, 2013. doi: 10.1089/ten.teb.2012.0437.

[65] Y. MANOME *et al.*, ‘Three-dimensional Cell Culture of Glioma and Morphological Comparison of Four Different Human Cell Lines’, *Anticancer Res*, vol. 30, no. 2, pp. 383–389, 2010, [Online]. Available: https://ar.iiarjournals.org/content/30/2/383

[66] T. Kojima *et al.*, ‘Dysfunction of epithelial permeability barrier induced by HMGB1 in 2.5D cultures of human epithelial cells’, *Tissue Barriers*, vol. 10, no. 2. Taylor and Francis Ltd., 2022. doi: 10.1080/21688370.2021.1972760.

[67] X. Zhang *et al.*, ‘Trifluoperazine, a novel autophagy inhibitor, increases radiosensitivity in glioblastoma by impairing homologous recombination’, *Journal of Experimental and Clinical Cancer Research*, vol. 36, no. 1, Sep. 2017, doi: 10.1186/s13046-017-0588-z.

[68] L. Xi *et al.*, ‘Antipsychotic Drug Trifluoperazine Suppresses Colorectal Cancer by Inducing G0/G1 Arrest and Apoptosis’, vol. 10, p. 1029, 2019, doi: 10.3389/fphar.2019.01029.

[69] J. Y. Jeong *et al.*, ‘Trifluoperazine and Its Analog Suppressed the Tumorigenicity of Non-Small Cell Lung Cancer Cell; Applicability of Antipsychotic Drugs to Lung Cancer Treatment’, *Biomedicines*, vol. 10, no. 5, May 2022, doi: 10.3390/biomedicines10051046.

[70] J. Park, J. Y. Jeong, and S. S. Kang, ‘COX-2 Acts as a Key Mediator of Trifluoperazine-induced Cell Death in U87MG Glioma Cells’, *Anticancer Res*, vol. 42, no. 12, 2022, doi: 10.21873/anticanres.16084.